Analysis of Head and Neck Cancer scRNA-seq Data Identified PRDM6 Promotes Tumor Progression by Modulating Immune Gene Expression

Authors

Zhenyu Wu[1], Thurbu Tshering Lepcha[1], Dawei Zhou[1], Zhixian He[2], Guillaume N. Fiches[1], Youngmin Park[1], Jinshan He[1], Jianwen Chen[1], K.A.S.N Shanaka [1], Steve Oghumu[1], Weiqiang Zhao[1], Anjun Ma[4], Qin Ma[4] , Jian Zhu[1,3,*] , Netty G. Santoso[1,*]

Affiliations

[1]Department of Pathology, College of Medicine, The Ohio State University, Columbus, OH 43210, USA

[2]Department of Microbiology, College of Arts and Sciences, The Ohio State University, Columbus, OH 43210, USA

[3]Department of Microbial Infection and Immunity, College of Medicine, The Ohio State University, Columbus, OH 43210, USA

[4]Department of Biomedical Informatics, College of Medicine, The Ohio State University, Columbus, OH 43210, USA

[*]To whom correspondence should be addressed: Netty Santoso (Netty.Santoso@osumc.edu) or Jian Zhu (Jian.Zhu@osumc.edu)

Keywords: head and neck cancer, PRDM6, IRG, scRNA-seq, HPV.

Abstract

Head and neck squamous cell carcinoma (HNSCC) is a biologically aggressive and heterogeneous group of cancers with limited treatment options for patients who do not respond to standard therapies. While HPV-related HNSCCs tend to show better therapeutic outcomes, we still had limited understanding of the immune mechanisms underlying these cancers. Immune-responsive genes (IRGs) have emerged as critical factors in regulating both tumor progression and immune response. Recent advances in single-cell RNA sequencing (scRNA-seq) and the development of cell-type specific regulon inference tools, such as IRIS3, have provided new insights into the tumor immune microenvironment. In this study, we leveraged the IRIS3 platform to analyze scRNA-seq data from HNSCC patient samples, identifying novel transcription factor (TF)-IRG networks that contribute to tumor proliferation and immune escape. Specifically, we identified PRDM6, a histone methyltransferase, possesses the previously unknown role in promoting tumor cell proliferation by inducing IRG expression. We further demonstrated that HPV viral oncoproteins (E6/E7) oncoproteins up-regulate the PRDM6 expression, which associates PRDM6 with HPV-positive HNSCC.

Introduction

Head and neck cancers (HNCs) represent the sixth most common cancer worldwide with the majority being head and neck squamous cell carcinoma (HNSCC). HNSCC typically arise from the mucosal linings of the upper aerodigestive tract (1, 2) and can be further classified according to its originating location, including the oral cavity, oropharynx, nasal cavity, paranasal sinuses, nasopharynx, larynx, and hypopharynx. Overall, HNSCC is highly heterogeneous and biologically aggressive, often associated with high rates of recurrence and mortality, especially at the advanced stages. Major risk factors of head and neck cancers include consumption of alcohol, exposure to nicotine, and infection with high-risk HPV (HPV16, 18) (*3*). Currently, the standard treatment of HNSCC includes surgery and/or chemo- and radiotherapy. Interestingly, HPV-associated HNSCC tends to have the better responses to treatments compared to HPV-negative ones (*4*), possibly due to its viral-related immunogenicity.

Despite of multiple anti-cancer treatment options, most of the locally advanced HNSCC cases still show poor responses with frequent recurrence. Immunotherapies have recently emerged as a promising alternative strategy to treat HNSCC considering that immune escape critically contributes to tumor initiation and progression (*5*). However, it is still at its early stage due to the lack of knowledge regarding the mechanism of immune regulation of HNSCC (*6*). Recently, it has been recognized that cancer cell-intrinsic genetic events profoundly modulate the tumor immune milieu and critically determine the outcome of immunotherapies (*7*). Immune-responsive genes (IRGs), thus, play a prominent role in not only controlling tumor initiation and progression but also participating in immune and inflammatory responses in tumor cells (*8, 9*). Moreover, several IRGs have been identified as tumor suppressors in various cancers, which directly impacts tumor growth (*10*).

Immunosurveillance plays an important role in controlling tumor initiation and progression. Malignant cells exploit various regulatory strategies to escape from immunosurveillance, including dysregulation of type I interferon (IFN) signaling (*11, 12*), immune checkpoint genes (*8*), as well as inflammatory responses (*13*) in tumor cells. Identification of TFs that govern IRG expression and depiction of related profound TF-IRG regulatory networks in tumor cells is critical to the understanding of tumor immunity, especially their own contribution directly from tumor cells. Through analysis of bulk RNA-seq datasets from The Cancer Genome Atlas (TCGA) consortium, differentially expressed IRGs and associated TF-IRG networks of HNSCC have been identified (*14, 15*). However, such bulk RNA-seq based analysis is unable to characterize cell type-specific IRG regulation.

The recent advance of single-cell RNA sequencing (scRNA-seq) technology enables the high-throughput analysis of gene expression at the resolution of individual cells. In our work, we developed a pipeline to perform the integrative analysis of multiple HNSCC scRNA-seq datasets and further the tumor cell-specific regulon inference analysis through the IRIS3 server (*16*). Results from our analysis provide a deeper understanding regarding the regulation of IRG expression in HNSCC malignant cells and the contribution of IRG dysregulation to tumor cell growth and immune response (*17*). In our studies, we utilized IRIS3 server to perform the integrative analysis of HNSCC scRNA-seq datasets, which led to the identification of tumor cell-specific regulons. Differentially expressed IRGs and novel transcription factor (TF)-IRG networks in tumor cells within the HNSCC microenvironment have been recognized. Here we report that PRDM6, a histone methyl-transferase (*18, 19*), which has never been implicated in HNSCC previously, regulate immune gene expression in HNSCC tumor cells, including interferon-stimulated genes (ISGs) ISG15 and IFITM1. Furthermore, we unraveled that HPV viral

oncoproteins (E6/E7) induces PRDM6 expression, indicating PRDM6's role in promoting HPV-positive HNSCC.

Results

IRIS3 analysis of HNSCC scRNA-seq data identified tumor cell-specific IRG-enriched regulons. We aimed to identify tumor cell-specific IRG-enriched regulons by using the publicly available HNSCC scRNA-seq datasets (**Table 1)**. Our pipeline consisted of initial quality-control (QC) step through Seurat to filter out low quality cells. A set of established cell biomarkers was used to annotate tumor cells and non-tumor cells (primarily immune or stromal cells). Any available metadata containing cell annotation were used for confirmation. Datasets with a low percentage of tumor cells (less than 5%) were excluded from this study to avoid imbalances (**Fig. 1A**). In total, scRNA-seq data from fourteen HNSCC patients were included for analysis. Patient information, including viral infection status and clinical cancer stages, was summarized (**Table 1**). We performed inference of cell type-specific regulons using the IRIS3 tool. By leveraging public ChIP-seq data and bi-clustering methods, IRIS3 effectively identified the cell type-specific regulons with high accuracy and specificity. We were able to discover 639 TF-associated regulons that were specific for tumor cells in HNSCC tissues (**Table S1**). Since we primarily focused on immune-related regulons, we further performed the hypergeometric test to sort the regulons, in which IRGs were enriched. In total, we identified 88 tumor cell-specific TFs in the IRG-enriched regulons that were present in at least one patient (**Table S2**). Among these, 10 TFs in $\geq$ ten patients, 24 TFs in $\geq$ five patients, and 52 TFs in $\geq$ two patients (**Fig. 1B**). We highlighted those 24 TFs that occurred in more than 5 patients (**Fig. 1C**). Pathway analysis revealed that the regulons that associate with these 24 TFs are predominantly enriched in metabolism regulation and RNA

processing (**Fig. S1A-C**), while IRG filtering indeed enriched the immune-related pathways for these regulons , including the response to viral infections and the NF-κB signaling (**Fig. S1A-C**). Among 24 TFs identified in more than five patients, several ones have been previously linked to HNSCC (*20-24*) (**Fig. 1D**), which validated the robustness of our IRIS3 analysis.

PRDM6 was recognized as a novel HNSCC-associated TF that regulates expression of IRGs in tumor cells. We focused on PRDM6 for further characterization since it has never been investigated in HNSCC. PRDM6 is a histone methyltransferase that regulates the methylation of H3K27 (*19*) and H4K20 (*25*). We identified 571 genes (**Table S3**) and 125 IRGs (**Fig. 2A**) in the PRDM6-associated regulon. To further investigate PRDM6's role in regulating IRGs, we investigated the global chromatin associations of PRDM6 by re-analyzing the public ChIP-seq datasets for human PRDM6 (**Fig. S2A,B**). We observed that the peak distributions of PRDM6 are consistent across two ChIP-seq datasets, GSE76496 (*26*) and GSE106058 (*27*), and that PRDM6 occupies largely near the introns and distal intergenic regions but around 14% peaks indeed near the promoter regions. We further re-analyzed the CUT&RUN data of PRDM6 (GSE243557) (*19*), which identified that more PRDM6 peaks enrich near the promoter regions (**Fig. S2C**). This study also provided the H3K27me3 CUT&RUN data in the scenario of PRDM6 overexpression. Our re-analysis showed that the distribution of H3K27me3 peaks (CUT&RUN) is similar to that of PRDM6 peaks (ChIP-seq), indicating that PRDM6 functions as a H3K27me3 methyltransferase (**Fig. S2D**). We also employed DeSeq2 to identify differentially expressed genes (DEGs) either upregulated or downregulated due to PRDM6 overexpression in human neuroepithelial stem cells (GSE243554). Pathway analysis of these DEGs using ClusterProfiler revealed that they are enriched in the pathways related to the viral life cycle and various developmental processes (**Fig. S2E,F**). Interestingly, scRNA-seq data indicated that PRDM6 expression occurs almost

exclusively in malignant cells while rarely in other cell types within the HNSCC tumors (**Fig. 2B**). We further determined the PRDM6 expression experimentally by using HNSCC cancer cell lines and tissue microarrays (TMAs). Our results showed that the PRDM6 expression is much higher in HNSCC cancer cell lines (CAL27, SCC9) in comparison to telomerase-immortalized normal human oral keratinocytes (OKF6/TERT-2, TIGK) at both protein and mRNA levels (**Fig. 2C,D**). We further confirmed that PRDM6 protein is present in TMAs of three HNSCC subjects (S1-S3) by using protein immunofluorescence staining assays (**Fig. 2E**). Overall, we could conclude that PRDM6 is a HNSCC-associated TF that preferentially expresses in HNSCC tumor cells.

PRDM6 promoted cell proliferation while suppressing immune gene expression of HNSCC tumor cells. As PRDM6 was shown to express in HNSCC tumor cells, we next determined whether PRDM6 contributes to their growth in vitro. We cloned the human PRDM6 cDNA in the pcDNA3.1 vector, which was transfected in CAL27 to generate cell clones. Our results revealed that the PRDM6- overexpressing CAL27 cell clones (1 and 2) consistently exhibit the higher cell viability and proliferation compared to vector only control by quantifying cellular ATP levels (**Fig. 3A**). Such effects were observed in these cells to be cultured continuously up to 5 days (**Fig. 3B**). We postulated that PRDM6 contributes to HNSCC tumor cell growth likely through dysregulation of immune gene expression based on our findings that PRDM6 is a HNSCC-associated TF that participates in the TF-IRG regulons identified from IRIS3 analysis. First, we observed that the expression of PRDM6 is moderately upregulated in CAL27 cells with IFN-α stimulation (**Fig. S3**). Second, we identified that depletion of PRDM6 by its siRNAs induces the expression of anti-tumor ISGs, ISG15 and IFITM1 (**Fig. 3C**). ISG15 was previously reported to inhibit the growth of tumor cells (*28, 29*) while inducing their cell death (*30*) by targeting the NF-kB and p53 signaling. The loss of IFITM1 was also shown to induce the cell cycle arrest (*31, 32*).

Third, we also showed that PRDM6 overexpression consistently results in the decrease of ISG15 and IFITM1 expression in CAL27 cell clones (1 and 2) **(Fig. 3D**). Overall, these results indicated that PRDM6 might participate in the type I IFN signaling and control the expression of antitumor ISGs in HNSCC tumor cells, thus promoting their proliferation and growth.

PRDM6 expression was upregulated by HPV-16 E6/E7 viral oncoproteins in HNSCC tumor cells. High-risk HPV (16 and 18) is a risk factor for HNSCC and specifically linked to oropharyngeal squamous cell carcinoma (OPSCC). HPV-encoded E6 and E7 (E6/E7) viral oncoproteins play a key role in driving the development and progression of HPV-associated cancers through various mechanisms (*33-35*). We next determined whether PRDM6 may participate in HPV E6/E7-mediated oral tumorigenesis. Our results showed that overexpression of HPV16 E6 and/or E7 oncoproteins indeed significantly increase PRDM6 expression in CAL27 cells by RT-qPCR analysis **(Fig. 4A)**. We further confirmed this finding in the telomerase-immortalized normal human foreskin keratinocytes (N/Tert-1) that harbor the HPV16 genome (N/Tert-1+HPV16), showing that PRDM6 expression is higher in N/Tert-1+HPV16 compared to the HPV16-native N/Tert-1cells **(Fig. 4B)**. Consistently, analysis of HNSCC bulk RNA-seq datasets from TCGA revealed that PRDM6 expression elevates in HPV-positive cases compared to HPV-negative ones (**Fig. 4C**), while expression of ISGs (ISG15, IFITM1) exhibits the opposite trend (**Fig. S4**). Overall, our findings implicated that HPV may target PRDM6 to suppress immune gene expression through induction of its expression by E6/E7 viral oncoproteins, thus promoting oral tumorigenesis (**Fig. 4D**).

Discussion

In this study, we integrated multiple datasets of HNSCC scRNA-seq with the aim to identify tumor cell-specific transcriptional/epigenetic regulators that control immune gene expression and tumor cell intrinsic immunity. Such efforts led to the identification of 639 tumor-specific TF regulons, including 88 IRG-enriched ones. Among them, the histone methyltransferase PRDM6 emerged as a top, previously un-investigated TF that may regulate the immune response in HNSCC tumor cells. We demonstrated that PRDM6 expression occurs almost exclusively in tumor cells of the clinic HNSCC tissues and that PRDM6 promotes proliferation and growth of HNSCC tumor cells *in vitro* while suppressing expression of anti-tumor ISGs (ISG15, IFITM1) by both loss- and gain-of-function approaches. We further identified that HPV16 E6/E7 oncoproteins upregulate PRDM6 expression in HNSCC tumor cells, which may link PRDM6 to HPV-induced oral oncogenesis.

TF gene regulatory networks as well as differentially expressed IRGs have been identified through analysis of HNSCC bulk RNA-seq datasets from TCGA (*36-38*). However, inherent limitations of bulk RNA-seq forbid the high-resolution characterizations of cellular heterogeneity within the tumor microenvironment, as gene expression levels across diverse types of cells in the tumor tissues are quantified with the setting that all types of cells are mixed together. Additionally, the regulon predictions primarily rely on the previous knowledge of benchmarked connections between TFs and their gene targets (*39, 40*). On the contrary, the scRNA-seq based transcriptomic profiling overcomes these limitations of bulk RNA-seq and enables the precise measurements of gene expressions that occur exclusively in malignant cells *vs* other types of cells in the tumor tissues, which permits us to annotate the HNSCC tumor cell-specific TF-IRG regulatory networks with the higher accuracy. IRIS3, powered by its unique bi-clustering algorithm and *de novo* motif prediction, has demonstrated its capability to identify the cell type-specific regulons with the

satisfying reproducibility and robustness (*16*), which enabled our successful identifications of 88 IRG-enriched TFs in the HNSCC tumor cells (**Fig. 1**).

We further characterized the histone methyltransferase PRDM6 as a potential TF that governs HNSCC tumor cell intrinsic immunity. Beyond the mere data mining, we experimentally verified that PRDM6 expresses in both HNSCC cancer cell lines and HNSCC clinic TMAs from multiple subjects (**Fig. 2**). We also demonstrated PRMD6's functions to promote proliferation and growth of HNSCC tumor cells, likely due to its activities to suppress expression of anti-tumor ISGs (**Fig. 3**). These results are overall consistent with the early findings that PRDM family of proteins possess the oncogenic potency, and regulate the tumor cell proliferation and differentiation (*18, 19, 25, 41, 42*). However, the exact underlying mechanisms for PRDM6 to drive development and progression of HNSCC still need further investigations in future. Nevertheless, it has been showcased that PRDM6 indeed targets the histone marks including H3K27 in medulloblastoma (*19*). It is thus plausible that PRDM6-induced H3K27 trimethylation (H3K27me3) likely leads to the suppression of immune gene expression in tumor cells.

We also reported that PRDM6 suppresses immune gene expression in HNSCC tumor cells, which is consistent with the previous studies on other members of PRDM proteins. In particular, PRDM1 is known to play a key role in immunosuppression in the tumor microenvironment. It has been shown that genetic ablation of PRDM1 is effective to stimulate antitumor T cell responses (*43*). On the contrary, the immunosuppressive functions of PRDM6 need to be further characterized. We did identify that PRDM6 expression is inducible in HNSCC tumor cells upon type I interferon stimulation, indicating that PRDM6 may be involved in tumor cell intrinsic immune signaling. There are also other clues. For example, it has been noted that PRDM6 protein associates with the histone methyltransferase G9a that is a critical regulator of inflammatory

responses as well as T cell functions (*44*). Overall, we provided the evidence that PRDM6 suppresses expression of antitumor ISGs, which may contribute to oral tumorigenesis.

HPV highly associates with HNSCC, especially OPSCC, as nearly 80% of oropharyngeal cancers in the United States are infected with the high-risk HPV (16 and 18) (3). HPV E6/E7 viral oncoproteins are critical to drive malignant transformation of normal oral epithelial cells by targeting key cellular pathways with multiple strategies, such as degradation of p53 protein (*45-47*), activation of human telomerase reverse transcriptase (hTERT) (*48, 49*), and disruption of retinoblastoma (Rb) protein (*50-52*). Our results suggested a new link that HPV E6/E7 may manipulate PRDM6 expression to antagonize the antitumor and antiviral immune responses as a previously unappreciated viral mechanism to promote oral tumorigenesis (**Fig. 4**). These findings would improve the fundamental understanding of HPV-associated HNSCC. However, it remains to be delineated how E6/E7 transcriptionally or epigenetically induces PRDM6 expression.

To summarize, our unbiased analysis of integrated HNSCC scRNA-seq datasets led to the identification of PRDM6 as a novel TF that governs the type I IFN signaling and immune gene expression and thus promotes proliferation and growth of tumor cells, while PRDM6 itself is also under control of HPV. These results would shed light in targeting PRDM6 for developing novel therapies to treat HNSCC. The potential immunosuppressive functions of PRDM6 would likely need to be interrupted or counteracted to boost antitumor immune responses, thus improving the efficacy of immunotherapies against HNSCC.

Material and Methods

Cells: CAL27 and SCC9 cells were cultured in DMEM supplemented with 10% FBS. OKF6/TERT-2 (*53*) and TIGK cells (*53*) were both cultured in keratinocyte serum-free medium

(K-sfm) with supplements (Thermo Scientific, CAT#17005042). Cell proliferation and growth was measured by using the ATP-based CellTiter-Glo Luminescent Cell Viability Assay (Promega, Cat. # G7572) following the manufacturer's instructions and analyzed by the Cytation 5 multimode reader (luminescent mode).

Quantitative PCR (qPCR): Total RNAs were extracted using the NucleoSpin RNA extraction kit (Macherey-Nagel, Cat. # 740955.250) following the protocols provided by the manufacturer. RNA samples were reverse transcribed to cDNAs using iScript (BioRad, Cat. # 1708891). Real-time qPCR was performed on a CFX96 instrument (BioRad), by mixing 5 ul (2x) SYBR Green Supermix (BioRad, Cat. # 1725214), 0.5 ul primer mix, and 4.5 ul cDNA template. Data were analyzed by using the ΔΔCt method with GAPDH as an internal control. All qPCR primers were listed in **Table S4**.

Protein immunoblotting: Protein immunoblotting was performed as previously described (*54*). The following antibodies were used: anti-PRDM6 (Invitrogen, Cat. # PA5-43659), anti-GAPDH (Santa Cruz Biotechnology, Cat. # sc-47724), anti-mouse-HRP (Cell Signaling technology, Cat. # 7076), anti-rabbit-HRP (Cell Signaling technology, Cat. # 7074). The membrane was washed and blocked with 5% BSA, followed by the incubation with the primary antibody (1:1000 dilution) in 10 ml of the antibody dilution buffer for overnight at 4 °C with shaking, and with the secondary anti-mouse or anti-rabbit antibody.

Transfection and electroporation: Turbofect reagents (Thermo Scientific, Cat. # R0531) were used for plasmid transfection following the manufacturer's recommendation as described previously (55). The pcDNA3.1 plasmid expressing the PRDM6 cDNA with FLAG tag at 3' end was purchased from GenScript. The pLXSN plasmid expressing FLAG-tagged E6 (Cat. # 52395), E7 (Cat. # 52396), E6/E7 (Cat. # 52394) were acquired from Addgene. siRNAs targeting PRDM6,

siPRDM6-1 (Cat. # s41097) and siPRDM6-2 (Cat. # s41098), were purchased from Invitrogen. For siRNA transfection in CAL27 and SCC9 cells, reverse transfection was performed using the Lipofectamine RNAiMAX (Invitrogen, Cat. # 13778100) as previously described (*9*).

Protein immunofluorescence: Paraffin-embedded HNSCC tissue slides were baked at 65°C for 30 mins, followed by deparaffinization in xylene (10 mins × 2), 100% ethanol (10 mins × 2), 95% ethanol (5 mins), 70% ethanol (1 min), 50% ethanol (1 min), and finally rehydrated in double-distilled water (5 minus). Antigen unmasking was performed using 2100 Retriever (Electron Microscopy Sciences, Cat. # 62700-10) with the Antigen Retrieval Buffer (100X Tris-EDTA Buffer, pH9.0; Abcam, Cat. # ab93684) for 2 hrs to complete the cycle and then cool down. To block non-specific binding, slides were incubated with 10% normal goat serum (NGS) in PBST (0.1% Tween-20 in PBS) for 2 hrs at room temperature (RT). Incubation with the primary antibody was carried out overnight at 4°C using rabbit anti-PRDM6 antibody with 5% NGS in PBST. Sections were then washed with PBST and incubated with Alexa Fluor 488-conjugated, anti-rabbit secondary antibody with 5% NGS for 1 hr at RT. Nuclear counterstaining was performed using Hoechst 33342 (1:5000 in D-PBS) for 15 mins at RT. Coverslips were mounted on slides using ProLong Glass Antifade Mountant (Invitrogen, Cat. # P36982) and dried in the dark overnight. Confocal images were acquired using the ZEISS LSM 700 Upright laser scanning confocal microscope and processed with ZEN imaging software (ZEISS).

Data analysis: Fastq files of the public bulk RNA-seq dataset (GSE243554) were obtained from GEO database and reanalyzed. Quality of raw reads was assessed by fastp (*56*). Reads were trimmed with adapters and aligned to the human genome (GRCh38.p14) with HISAT2 aligner. Uniquely aligned reads were submitted as inputs for mapping to gencode.v39 annotation. For identification of DEGs, DESeq2 was run with raw read counts obtained from FeatureCounts.

Adjusted p value =< 0.05 and fold change >= 2 were used to filter for DEGs. For re-analysis of HNSCC scRNA-seq datasets, expression matrix was downloaded from GEO with the accession number GSE103322 (*57*), GSE150430 (*58*), GSE150321 (*59*), GSE162025 (*60*), and GSE150825 (*61*). Low-quality cells or empty droplets were filtered out based on the number of unique genes, the total number of molecules, and the percentage of mitochondrial reads detected in each cell. Normalization and scaling of cell clustering and visualization were performed using SeuratV4.0 (*62*). Cell identity was assigned based on the metadata and marker genes. Raw data of the public ChIP-seq datasets (GSE76496, GSE106058) were acquired from GEO and processed with ENCODE ChIP-seq-pipeline2. PRDM6 and H3K27me3 CUT&RUN peaks from GSE243557 were visualized using IGV. The code used for above analyses was deposited at github: https://github.com/ZhenyuWu-OSU

Statistics: Statistical analyses of experiment results were performed by using the unpaired, two-tailed Student's *t* test or the one-way analysis of variance (ANOVA) in Graphpad PRISM 9.0 package. Variables were compared among all tested groups, and the P values below 0.05 were considered as statistically significant.

Acknowledgment

We would like to thank Dr. James G. Rheinwald for providing the OKF6/TERT-2 cells, and Dr. Jens Kreth (Oregon Health & Science University) for the TIGK cells. We appreciate the supports from Drs. Yuzhou Chang and Cankun Wang for performing the IRIS3 analysis. We also appreciate the supports from Dr. Meng Wang (Research Institute at Nationwide Children's

Hospital) to establish the analytic pipelines of ChIP-seq data. This study was supported by NIH research grants R01CA260690 to N.S.; R01MH134402, R01DA059538, R56AI181631 to J.Z.

1. C. R. Leemans, P. J. F. Snijders, R. H. Brakenhoff, The molecular landscape of head and neck cancer. *Nature reviews. Cancer* **18**, 269-282 (2018).
2. O. A. Elkashty, R. Ashry, S. D. Tran, Head and neck cancer management and cancer stem cells implication. *Saudi Dent J* **31**, 395-416 (2019).
3. M. E. Sabatini, S. Chiocca, Human papillomavirus as a driver of head and neck cancers. *British Journal of Cancer* **122**, 306-314 (2020).
4. A. K. Chaturvedi *et al.*, Human papillomavirus and rising oropharyngeal cancer incidence in the United States. *Journal of clinical oncology* **29**, 4294 (2011).
5. P. Economopoulou, I. Kotsantis, A. Psyrri, The promise of immunotherapy in head and neck squamous cell carcinoma: combinatorial immunotherapy approaches. *ESMO Open* **1**, e000122 (2016).
6. S. Miyauchi *et al.*, Immune Modulation of Head and Neck Squamous Cell Carcinoma and the Tumor Microenvironment by Conventional Therapeutics. *Clin Cancer Res* **25**, 4211-4223 (2019).
7. M. D. Wellenstein, K. E. de Visser, Cancer-Cell-Intrinsic Mechanisms Shaping the Tumor Immune Landscape. *Immunity* **48**, 399-416 (2018).
8. W. Chen, M. Ou, D. Tang, Y. Dai, W. Du, Identification and Validation of Immune-Related Gene Prognostic Signature for Hepatocellular Carcinoma. *Journal of Immunology Research* **2020**, 5494858 (2020).
9. G. N. Fiches *et al.*, Profiling of immune related genes silenced in EBV-positive gastric carcinoma identified novel restriction factors of human gammaherpesviruses. *PLoS Pathog* **16**, e1008778 (2020).
10. D. Xiong, Y. Wang, M. You, Tumor intrinsic immunity related proteins may be novel tumor suppressors in some types of cancer. *Sci Rep* **9**, 10918 (2019).
11. J. Dubrot *et al.*, In vivo CRISPR screens reveal the landscape of immune evasion pathways across cancer. *Nature Immunology* **23**, 1495-1506 (2022).
12. E. Toufektchan *et al.*, Intratumoral TREX1 Induction Promotes Immune Evasion by Limiting Type I IFN. *Cancer Immunology Research* **12**, 673-686 (2024).
13. X. Yang *et al.*, Head and Neck Cancers Promote an Inflammatory Transcriptome through Coactivation of Classic and Alternative NF-κB Pathways. *Cancer Immunol Res* **7**, 1760-1774 (2019).
14. L. Li *et al.*, Comprehensive immunogenomic landscape analysis of prognosis-related genes in head and neck cancer. *Sci Rep* **10**, 6395 (2020).
15. Y. Yao *et al.*, Prognostic value of novel immune-related genomic biomarkers identified in head and neck squamous cell carcinoma. *J Immunother Cancer* **8**, (2020).
16. A. Ma *et al.*, IRIS3: integrated cell-type-specific regulon inference server from single-cell RNA-Seq. *Nucleic Acids Research* **48**, W275-W286 (2020).
17. J.-H. Choi *et al.*, Single-cell transcriptome profiling of the stepwise progression of head and neck cancer. *Nature Communications* **14**, 1055 (2023).
18. C. A. Davis *et al.*, PRISM/PRDM6, a transcriptional repressor that promotes the proliferative gene program in smooth muscle cells. *Mol Cell Biol* **26**, 2626-2636 (2006).
19. C. Schmidt *et al.*, PRDM6 promotes medulloblastoma by repressing chromatin accessibility and altering gene expression. *Sci Rep* **14**, 16074 (2024).

20. X. B. Liu, J. Wang, K. Li, X. N. Fan, Sp1 promotes cell migration and invasion in oral squamous cell carcinoma by upregulating Annexin A2 transcription. *Mol Cell Probes* **46**, 101417 (2019).
21. J. Fang *et al.*, Knockdown of zinc finger protein, X-linked (ZFX) inhibits cell proliferation and induces apoptosis in human laryngeal squamous cell carcinoma. *Mol Cell Biochem* **360**, 301-307 (2012).
22. X. Li *et al.*, Wilms' tumor gene 1 regulates p63 and promotes cell proliferation in squamous cell carcinoma of the head and neck. *BMC Cancer* **15**, 342 (2015).
23. Z. Chen *et al.*, PRKD3 promotes malignant progression of OSCC by downregulating KLF16 expression. *Eur Rev Med Pharmacol Sci* **24**, 12709-12716 (2020).
24. V. Sailer *et al.*, PITX2 and PANCR DNA methylation predicts overall survival in patients with head and neck squamous cell carcinoma. *Oncotarget* **7**, 75827-75838 (2016).
25. Y. Wu *et al.*, PRDM6 is enriched in vascular precursors during development and inhibits endothelial cell proliferation, survival, and differentiation. *Journal of Molecular and Cellular Cardiology* **44**, 47-58 (2008).
26. F. W. Schmitges *et al.*, Multiparameter functional diversity of human C2H2 zinc finger proteins. *Genome Res* **26**, 1742-1752 (2016).
27. I. Dunham *et al.*, An integrated encyclopedia of DNA elements in the human genome. *Nature* **489**, 57-74 (2012).
28. M. J. Zhou *et al.*, ISG15 inhibits cancer cell growth and promotes apoptosis. *Int J Mol Med* **39**, 446-452 (2017).
29. T. Qu *et al.*, ISG15 induces ESRP1 to inhibit lung adenocarcinoma progression. *Cell Death & Disease* **11**, 511 (2020).
30. H. Mao *et al.*, Interferon-stimulated gene 15 induces cancer cell death by suppressing the NF-κB signaling pathway. *Oncotarget* **7**, 70143-70151 (2016).
31. L. Zhang *et al.*, Knockdown of interferon-induced transmembrane protein 1 inhibited proliferation, induced cell cycle arrest and apoptosis, and suppressed MAPK signaling pathway in pancreatic cancer cells. *Biosci Biotechnol Biochem* **84**, 1603-1613 (2020).
32. W. Zheng *et al.*, Down-regulation of IFITM1 and its growth inhibitory role in cervical squamous cell carcinoma. *Cancer Cell International* **17**, 88 (2017).
33. A. Lifsics *et al.*, The Role of the p16 and p53 Tumor Suppressor Proteins and Viral HPV16 E6 and E7 Oncoproteins in the Assessment of Survival in Patients with Head and Neck Cancers Associated with Human Papillomavirus Infections. *Cancers (Basel)* **15**, (2023).
34. T. de Bakker *et al.*, Restoring p53 Function in Head and Neck Squamous Cell Carcinoma to Improve Treatments. *Front Oncol* **11**, 799993 (2021).
35. E. Peta *et al.*, HPV16 E6 and E7 upregulate the histone lysine demethylase KDM2B through the c-MYC/miR-146a-5p axys. *Oncogene* **37**, 1654-1668 (2018).
36. Comprehensive genomic characterization of head and neck squamous cell carcinomas. *Nature* **517**, 576-582 (2015).
37. M. Xiao *et al.*, Complex interaction and heterogeneity among cancer stem cells in head and neck squamous cell carcinoma revealed by single-cell sequencing. *Front Immunol* **13**, 1050951 (2022).
38. Y. Chen, Z. Y. Li, G. Q. Zhou, Y. Sun, An Immune-Related Gene Prognostic Index for Head and Neck Squamous Cell Carcinoma. *Clin Cancer Res* **27**, 330-341 (2021).

39. R. Janky *et al.*, iRegulon: from a gene list to a gene regulatory network using large motif and track collections. *PLoS Comput Biol* **10**, e1003731 (2014).
40. N. Tomar, A. Mishra, N. Mrinal, B. Jayaram, Onco-Regulon: an integrated database and software suite for site specific targeting of transcription factors of cancer genes. *Database (Oxford)* **2016**, (2016).
41. A. Casamassimi *et al.*, Multifaceted Role of PRDM Proteins in Human Cancer. *Int J Mol Sci* **21**, (2020).
42. S. Mzoughi, Y. X. Tan, D. Low, E. Guccione, The role of PRDMs in cancer: one family, two sides. *Current Opinion in Genetics & Development* **36**, 83-91 (2016).
43. T. Yoshikawa *et al.*, Genetic ablation of PRDM1 in antitumor T cells enhances therapeutic efficacy of adoptive immunotherapy. *Blood* **139**, 2156-2172 (2022).
44. A. Muneer *et al.*, Non-canonical function of histone methyltransferase G9a in the translational regulation of chronic inflammation. *Cell Chem Biol* **30**, 1525-1541.e1527 (2023).
45. J. T. Thomas, L. A. Laimins, Human papillomavirus oncoproteins E6 and E7 independently abrogate the mitotic spindle checkpoint. *J Virol* **72**, 1131-1137 (1998).
46. D. A. Thompson *et al.*, The human papillomavirus-16 E6 oncoprotein decreases the vigilance of mitotic checkpoints. *Oncogene* **15**, 3025-3035 (1997).
47. D. Martinez-Zapien *et al.*, Structure of the E6/E6AP/p53 complex required for HPV-mediated degradation of p53. *Nature* **529**, 541-545 (2016).
48. L. Gewin, H. Myers, T. Kiyono, D. A. Galloway, Identification of a novel telomerase repressor that interacts with the human papillomavirus type-16 E6/E6-AP complex. *Genes & development* **18**, 2269-2282 (2004).
49. T. Veldman, X. Liu, H. Yuan, R. Schlegel, Human papillomavirus E6 and Myc proteins associate in vivo and bind to and cooperatively activate the telomerase reverse transcriptase promoter. *Proceedings of the National Academy of Sciences* **100**, 8211-8216 (2003).
50. M. Tommasino, L. Crawford, Human papillomavirus E6 and E7: proteins which deregulate the cell cycle. *Bioessays* **17**, 509-518 (1995).
51. M. Tommasino, in *Seminars in cancer biology*. (Elsevier, 2014), vol. 26, pp. 13-21.
52. E. Reinstein, M. Scheffner, M. Oren, A. Ciechanover, A. Schwartz, Degradation of the E7 human papillomavirus oncoprotein by the ubiquitin-proteasome system: targeting via ubiquitination of the N-terminal residue. *Oncogene* **19**, 5944-5950 (2000).
53. M. A. Dickson *et al.*, Human keratinocytes that express hTERT and also bypass a p16(INK4a)-enforced mechanism that limits life span become immortal yet retain normal growth and differentiation characteristics. *Mol Cell Biol* **20**, 1436-1447 (2000).
54. D. Zhou *et al.*, Inhibition of Polo-like kinase 1 (PLK1) facilitates the elimination of HIV-1 viral reservoirs in CD4⁺ T cells ex vivo. *Science Advances* **6**, eaba1941 (2020).
55. G. N. Fiches *et al.*, Polyamine biosynthesis and eIF5A hypusination are modulated by the DNA tumor virus KSHV and promote KSHV viral infection. *PLoS Pathog* **18**, e1010503 (2022).
56. S. Chen, Y. Zhou, Y. Chen, J. Gu, fastp: an ultra-fast all-in-one FASTQ preprocessor. *Bioinformatics* **34**, i884-i890 (2018).

57. A. R. Cillo *et al.*, Immune Landscape of Viral- and Carcinogen-Driven Head and Neck Cancer. *Immunity* **52**, 183-199.e189 (2020).
58. Y. P. Chen *et al.*, Single-cell transcriptomics reveals regulators underlying immune cell diversity and immune subtypes associated with prognosis in nasopharyngeal carcinoma. *Cell Res* **30**, 1024-1042 (2020).
59. L. Song *et al.*, Cellular heterogeneity landscape in laryngeal squamous cell carcinoma. *Int J Cancer* **147**, 2879-2890 (2020).
60. Y. Liu *et al.*, Tumour heterogeneity and intercellular networks of nasopharyngeal carcinoma at single cell resolution. *Nat Commun* **12**, 741 (2021).
61. L. Gong *et al.*, Comprehensive single-cell sequencing reveals the stromal dynamics and tumor-specific characteristics in the microenvironment of nasopharyngeal carcinoma. *Nat Commun* **12**, 1540 (2021).
62. Y. Hao *et al.*, Integrated analysis of multimodal single-cell data. *Cell* **184**, 3573-3587.e3529 (2021).

Table 1. The list of HNSCC scRNA-seq datasets used in the study. The number and percentage of tumor cells were provided for each of 14 HNSCC patients. Certain patients were excluded from the analysis due to either insufficient number of tumor cells or low percentage.

Data Source	Cancer Type	Tumor Cells number	Tumor cells Ratio (>5%)	Patient ID
GSE103322	HNSCC	2215	37.5%	N/A
GSE150430	NPC	1834	82.7%	P01
		92	28.8%	P04
		170	9.2%	P05
		233	10.5%	P06
		1975	76.3%	P11
		1069	55.9%	P12
		1501	59.5%	P13
		214	8.6%	P14
GSE162025	NPC	480	5.0%	P02
		487	7.5%	P13
		1132	15.4%	P16
GSE150321	LSCC	5777	54.0%	P01
		1321	34.0%	P02

Figure Legends

Figure 1. Identification of tumor cell-specific TF-IRG regulons through analysis of HNSCC scRNA-seq data. (A) The workflow utilized to identify tumor cell-specific TF-IRG regulons of HNSCC. HNSCC scRNA-seq datasets were collected and checked for quality. Clustering and annotation of single-cell data were performed by using Seurat. Cell-type specific regulons were identified by using the IRIS3 tool. (B) There are in total 88 TFs identified to regulate the expression of IRGs in HNSCC tumor cells. TFs were grouped according to their occurrence in multiple patients. (C) The 24 TFs identified in at least 5 patients were listed. (Red: TFs identified from $\geq$ 10 HNSCC patients; Green: TFs $\geq$ 5 HNSCC patients.) (D) Visualization of regulatory connections between 24 TFs and selected IRGs by using cytoscape (IRG: blue; TF: orange).

Figure 2. Characterization of PRDM6 as a HSNCC tumor cell-specific TF that regulates IRG expression. (A) PRDM6-IRG regulon identified by using the IRIS3 tool (IRG: blue; PRDM6: orange). (B) Expression level of PRDM6 across multiple cell types in HNSCC tumors from the public scRNA-seq dataset (GSE103322). Tumor and immune cells were annotated based on the expression of marker genes and internal labels. (C) Protein expression of PRDM6 in HNSCC cancer cell lines (CAL27, SCC9) as well as telomerase-immortalized normal human oral keratinocytes (OKF6/TERT-2, TIGK) was measured by protein immunoblotting analysis. GAPDH was used as the loading control. (D) The RNAs extracted from the above cells (C) were subjected to RT-qPCR analysis of PRDM6 transcript with normalization to GAPDH. (E) Expression of PRDM6 in tissue microarrays of three HNSCC subjects (S1-S3) was measured by protein immunofluorescence analysis with nuclei stained with Hoechst (PRDM6: green; nuclei: blue; scale bar: 50 μm). Results were calculated from two independent experiments and presented as mean ± SD. (*$p < 0.05$, **$p < 0.01$, ***$p < 0.001$, ****$p < 0.0001$, Student's *t* test).

Figure 3. Functions of PRDM6 to promote growth of HNSCC tumor cells while suppress expression of anti-tumor ISGs. (A) The pcDNA vector expressing FLAG-PRDM6 was transfected in CAL27 cells to generate PRDM6-overexpressing cell clones (1 and 2). The empty vector (EV) was also transfected in CAL27 cells to generate a negative control. A portion of above cells was harvested for RNA extraction and RT-qPCR analysis of PRDM6 transcripts with normalization to GAPDH (left panel). The rest of cells was subjected to ATP-based cell viability analysis (right panel). (B) CAL27 cells transfected with the pcDNA vector expressing FLAG-PRDM6 (clones 1 and 2) or EV were cultured continuously. A portion of cells was harvested at the indicated timepoints and subjected to cell viability analysis. (C) siRNAs targeting PRDM6 (si1 and si2) or non-targeting control (siNT) were transfected in CAL27 cells. RNAs were extracted and subjected to RT-qPCR analysis of PRDM6 or ISG transcripts (ISG15, IFITM1) with normalization to GAPDH. (D) CAL27 cells transfected with the pcDNA vector expressing FLAG-PRDM6 (clones 1 and 2) or EV were subjected to RNA extractions and RT-qPCR analysis of ISG transcripts (ISG15, IFITM1) with normalization to GAPDH. Results were calculated from two independent experiments and shown as mean ± SD. (*$p < 0.05$, **$p < 0.01$, ***$p < 0.001$, ****$p < 0.0001$, Student's *t* test).

Figure 4. Induction of PRDM6 expression by HPV-16 E6/E7 viral oncoproteins in HNSCC tumor cells. (A) The pLXSN vector expressing FLAG-E6 (left panel), FLAG-E7 (middle panel), FLAG-E6/E7 (right panel), or the or empty vector (EV) was transfected in Cal27 cells. RNAs were extracted and subjected to RT-qPCR analysis of PRDM6 or E6/E7 transcripts with normalization to GAPDH. (B) The telomerase-immortalized normal human foreskin keratinocytes with or without HPV-16 genome, N/Tert-1+HPV16 or N/Tert-1 cells, were subjected to RNA extractions and RT-qPCR analysis of PRDM6 transcripts with normalization to GAPDH. (C)

HNSCC bulk RNA-seq datasets from TCGA were re-analyzed. Expression levels of PRDM6 in HPV-positive and negative (HPV+/-) HNSCC patients were compared. (D) A working model described that HPV may induce PRDM6 expression by E6/E7 viral oncoproteins to suppress expression of anti-tumor ISGs and thus promote development of HNSCC. Results were calculated from three independent experiments and shown as mean ± SD. (*$p < 0.05$, **$p < 0.01$, ***$p < 0.001$, ****$p < 0.0001$, Student's t test).

Supplemental Materials

Figure S1. (A) Visualization of the TF-associated regulons for those TFs identified from at least 5 HNSCC patients. In total, 4,560 genes (blue) were predicted to under regulation of 24 TFs (orange), resulting in 36,696 predicted regulatory interactions between TFs and gene targets. TFs were clustered according to their eccentricity using Cytoscape. (B) Visualization of the TF-associated, IRG-enriched regulons for 24 TFs. The 4,560 genes were further filtered with the IRGs. In total, 1,636 IRGs (green) were predicted to under regulation of 24 TFs (red), resulting in 12,029 predicted regulatory interactions between TFs and IRGs. TFs were clustered according to their eccentricity using Cytoscape. (C) Pathway analysis was conducted for genes regulated by 24 TFs using ClusterProfiler, showing the enrichment of RNA processing pathway for general gene targets or viral response, transcription, and translation regulation pathways for IRGs, respectively.

Figure S2. (A-C) Public PRDM6 ChIP-seq datasets GSE106058 (A) and GSE76496 (B), as well as PRDM6 CUT&RUN dataset GSE243557 (C) were collected for re-analysis. The distribution of PRDM6 binding peaks across human genomes was visualized using Chipseeker. (C) Re-analysis of public PRDM6 ChIP-seq data (GSE76496) and H3K27me3 CUT&RUN data (GSE243557) demonstrated the similar distribution of PRDM6 and H3K27me3 bindings peaks. (E, F) Pathway analysis of the upregulated (F) and downregulated (G) gene expression in human neuroepithelial stem (NES) cells with PRDM6 overexpression (GSE243554).

Figure S3. CAL27 cells were treated with IFN-α at the indicated doses. RNAs were extracted and subjected to RT-qPCR analysis of PRDM6 transcripts with normalization to GAPDH.

Figure S4. HNSCC bulk RNA-seq datasets from TCGA were re-analyzed. Expression levels of ISG15 and IFITM1 in HPV+/- HNSCC patients were compared.

Table S1. List of 639 TFs that regulate gene expression in HNSCC tumor cells.

Table S2. List of 88 TFs that target IRG expression in HNSCC tumor cells identified from at least one patient.

Table S3. List of 571 genes under regulation of PRDM6.

Table S4. qPCR primers used in the study.

Figure 1

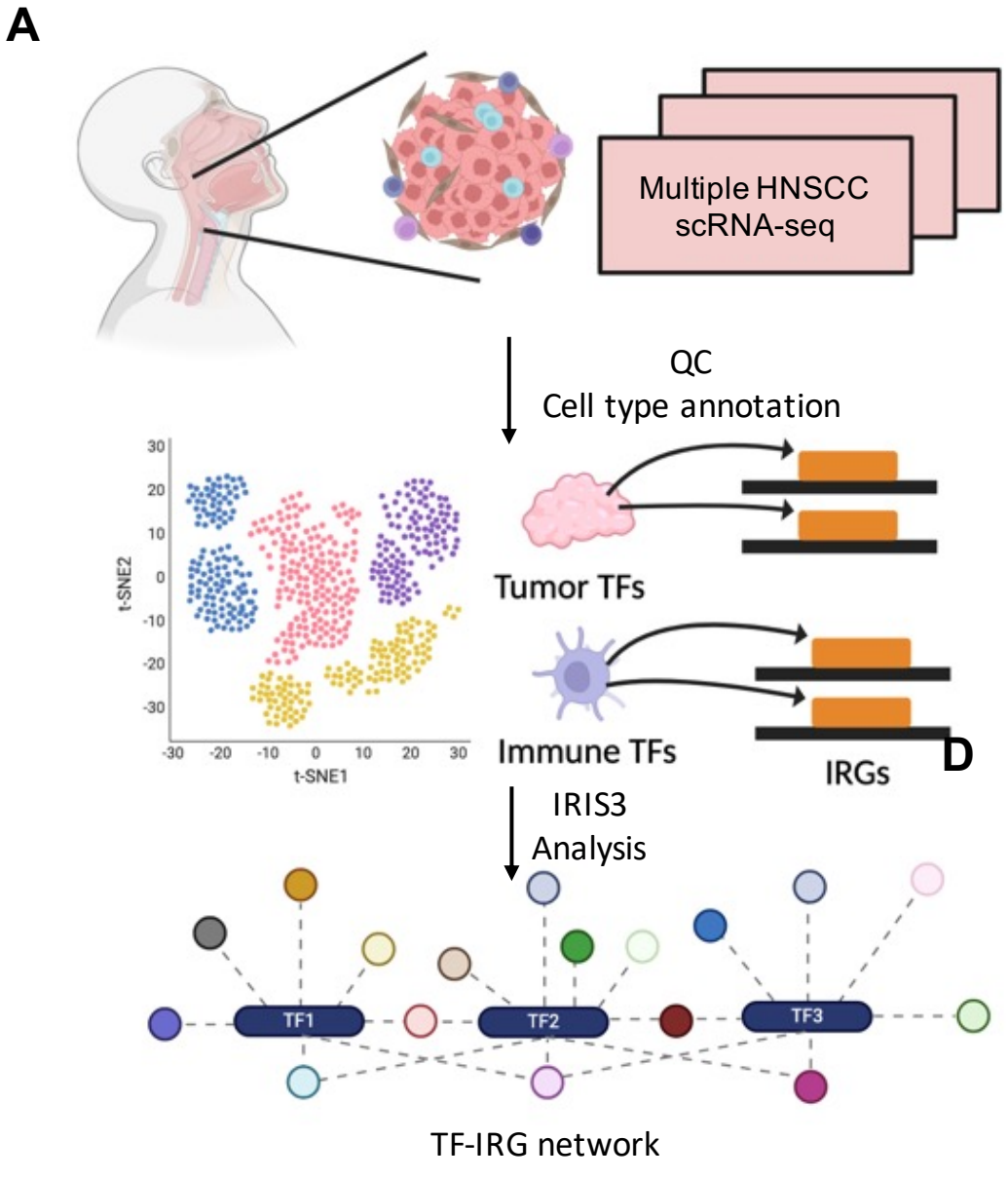

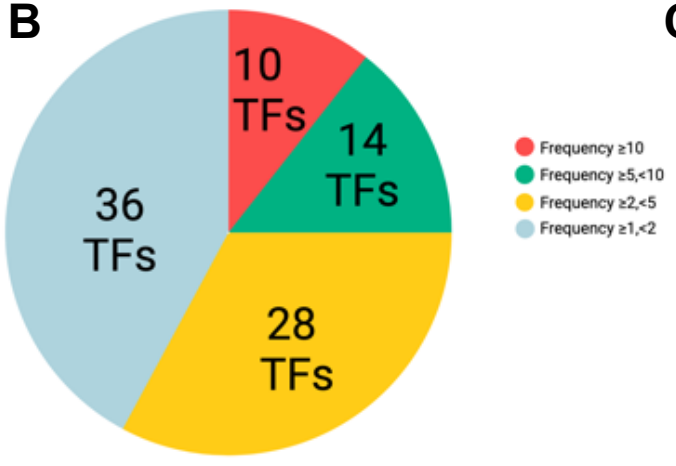

C

PATZ1	CPEB1	FOXJ3
SP1	TBX15	KLF12
SP2	RXRA	KLF3
SP3	SP4	PRDM6
VEZF1	AP2B	SALL4
ZFX	KLF16	TBX1
WT1	PITX2	ZN467
ZN770		
ETS2		
MAZ		

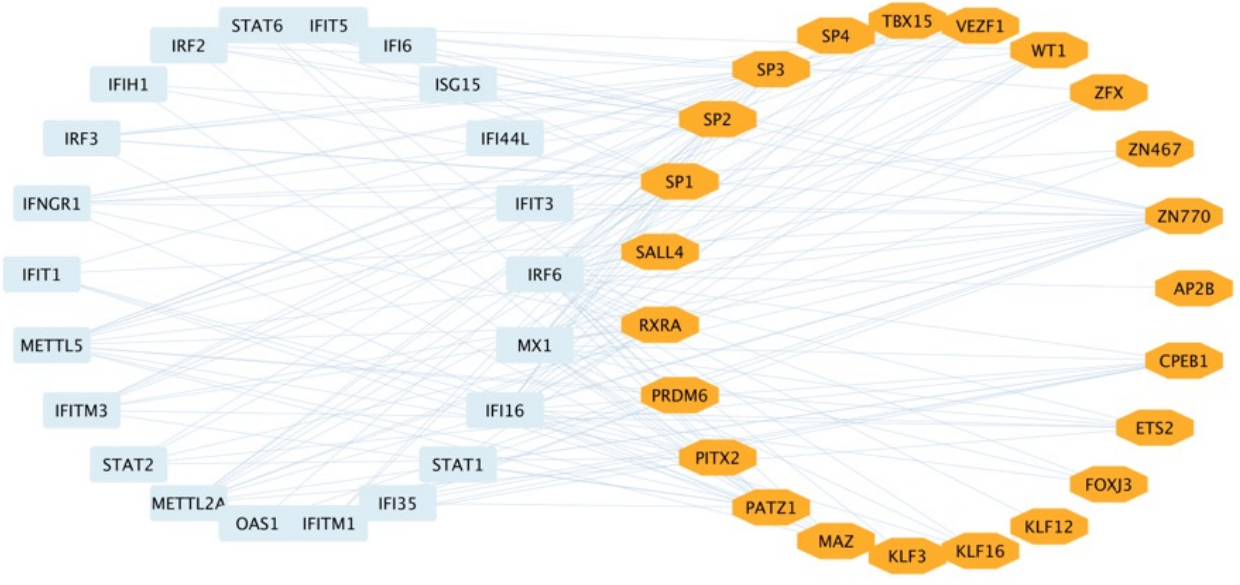

Figure 2

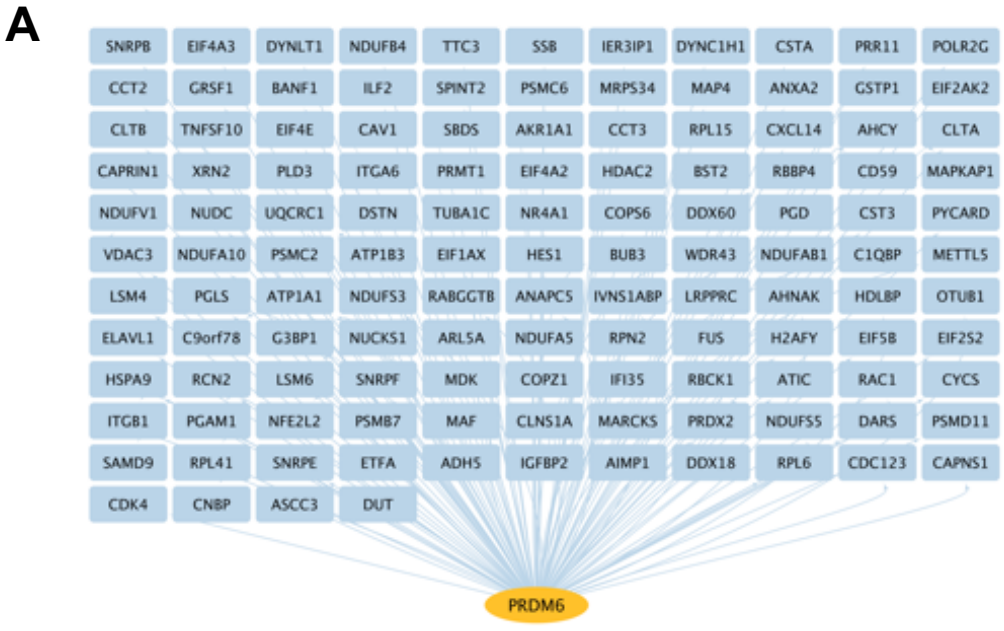
A
SNRPB EIF4A3 DYNLT1 NDUFB4 TTC3 SSB IER3IP1 DYNC1H1 CSTA PRR11 POLR2G
CCT2 GRSF1 BANF1 ILF2 SPINT2 PSMC6 MRPS34 MAP4 ANXA2 GSTP1 EIF2AK2
CLTB TNFSF10 EIF4E CAV1 SBDS AKR1A1 CCT3 RPL15 CXCL14 AHCY CLTA
CAPRIN1 XRN2 PLD3 ITGA6 PRMT1 EIF4A2 HDAC2 BST2 RBBP4 CD59 MAPKAP1
NDUFV1 NUDC UQCRC1 DSTN TUBA1C NR4A1 COPS6 DDX60 PGD CST3 PYCARD
VDAC3 NDUFA10 PSMC2 ATP1B3 EIF1AX HES1 BUB3 WDR43 NDUFAB1 C1QBP METTL5
LSM4 PGLS ATP1A1 NDUFS3 RABGGTB ANAPC5 IVNS1ABP LRPPRC AHNAK HDLBP OTUB1
ELAVL1 C9orf78 G3BP1 NUCKS1 ARL5A NDUFA5 RPN2 FUS H2AFY EIF5B EIF2S2
HSPA9 RCN2 LSM6 SNRPF MDK COPZ1 IFI35 RBCK1 ATIC RAC1 CYCS
ITGB1 PGAM1 NFE2L2 PSMB7 MAF CLNS1A MARCKS PRDX2 NDUFS5 DARS PSMD11
SAMD9 RPL41 SNRPE ETFA ADH5 IGFBP2 AIMP1 DDX18 RPL6 CDC123 CAPNS1
CDK4 CNBP ASCC3 DUT
PRDM6

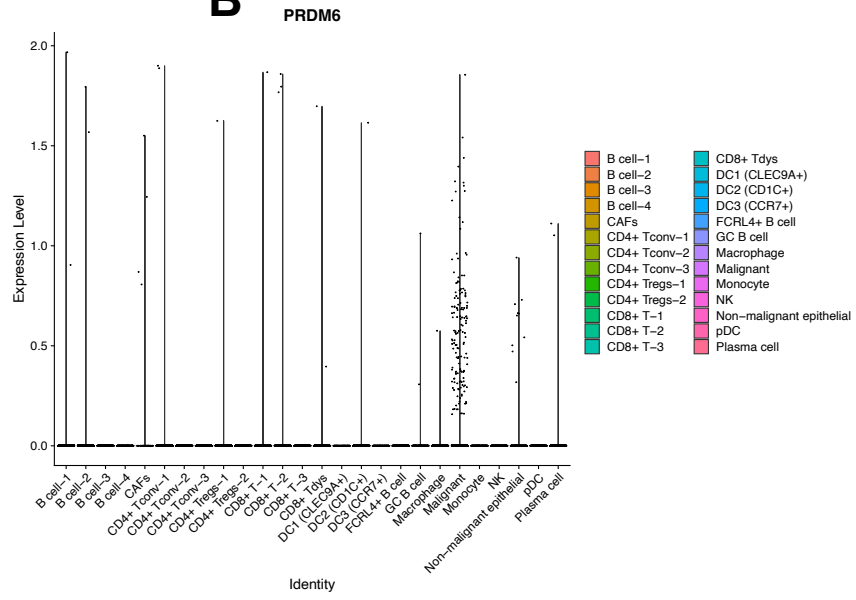
B
PRDM6
Expression Level
2.0
1.5
1.0
0.5
0.0
B cell−1
B cell−2
B cell−3
B cell−4
CAFs
CD4+ Tconv−1
CD4+ Tconv−2
CD4+ Tconv−3
CD4+ Tregs−1
CD4+ Tregs−2
CD8+ T−1
CD8+ T−2
CD8+ T−3
CD8+ Tdys
DC1 (CLEC9A+)
DC2 (CD1C+)
DC3 (CCR7+)
FCRL4+ B cell
GC B cell
Macrophage
Malignant
Monocyte
NK
Non−malignant epithelial
pDC
Plasma cell
Identity

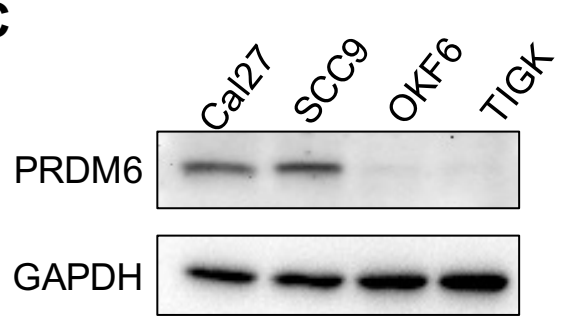
C
Cal27
SCC9
OKF6
TIGK
PRDM6
GAPDH

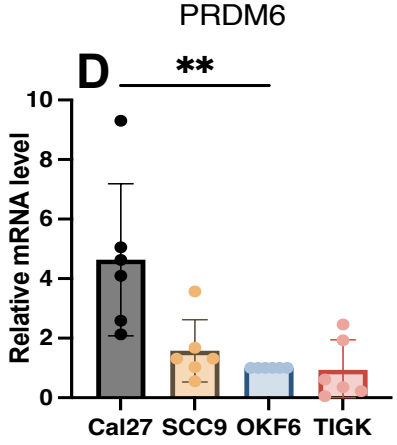
PRDM6
D
**
Relative mRNA level
10
8
6
4
2
0
Cal27
SCC9
OKF6
TIGK

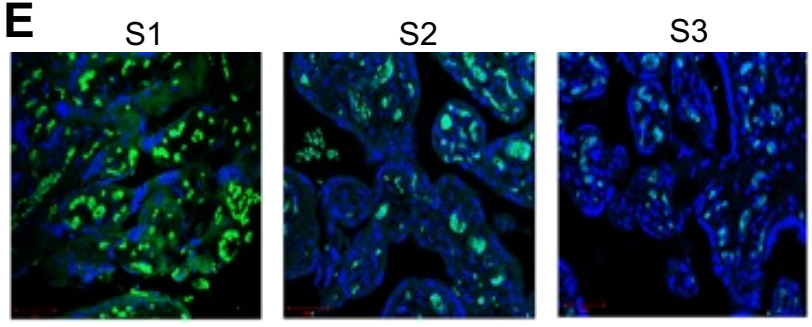
E
S1
S2
S3

Figure 3

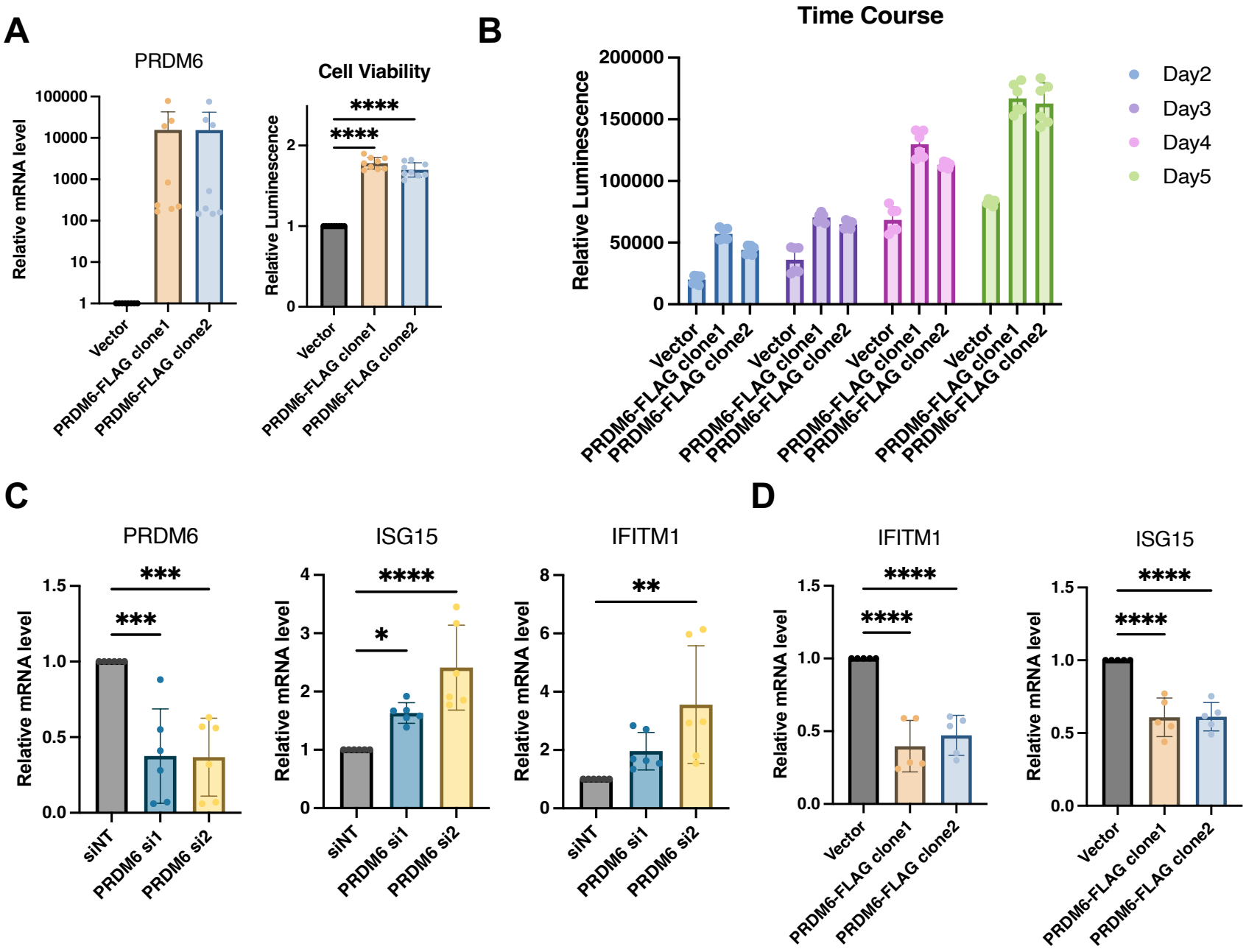
A
PRDM6
Relative mRNA level
100000
10000
1000
100
10
1
Vector
PRDM6-FLAG clone1
PRDM6-FLAG clone2
Cell Viability
Relative Luminescence
****
****
2
1
0
Vector
PRDM6-FLAG clone1
PRDM6-FLAG clone2
B
Time Course
Relative Luminescence
200000
150000
100000
50000
0
Day2
Day3
Day4
Day5
Vector
PRDM6-FLAG clone1
PRDM6-FLAG clone2
C
PRDM6
Relative mRNA level
***
***
1.5
1.0
0.5
0.0
siNT
PRDM6 si1
PRDM6 si2
ISG15
Relative mRNA level
****
*
4
3
2
1
0
siNT
PRDM6 si1
PRDM6 si2
IFITM1
Relative mRNA level
**
8
6
4
2
0
siNT
PRDM6 si1
PRDM6 si2
D
IFITM1
Relative mRNA level
****
****
1.5
1.0
0.5
0.0
Vector
PRDM6-FLAG clone1
PRDM6-FLAG clone2
ISG15
Relative mRNA level
****
****
1.5
1.0
0.5
0.0
Vector
PRDM6-FLAG clone1
PRDM6-FLAG clone2

Figure 4

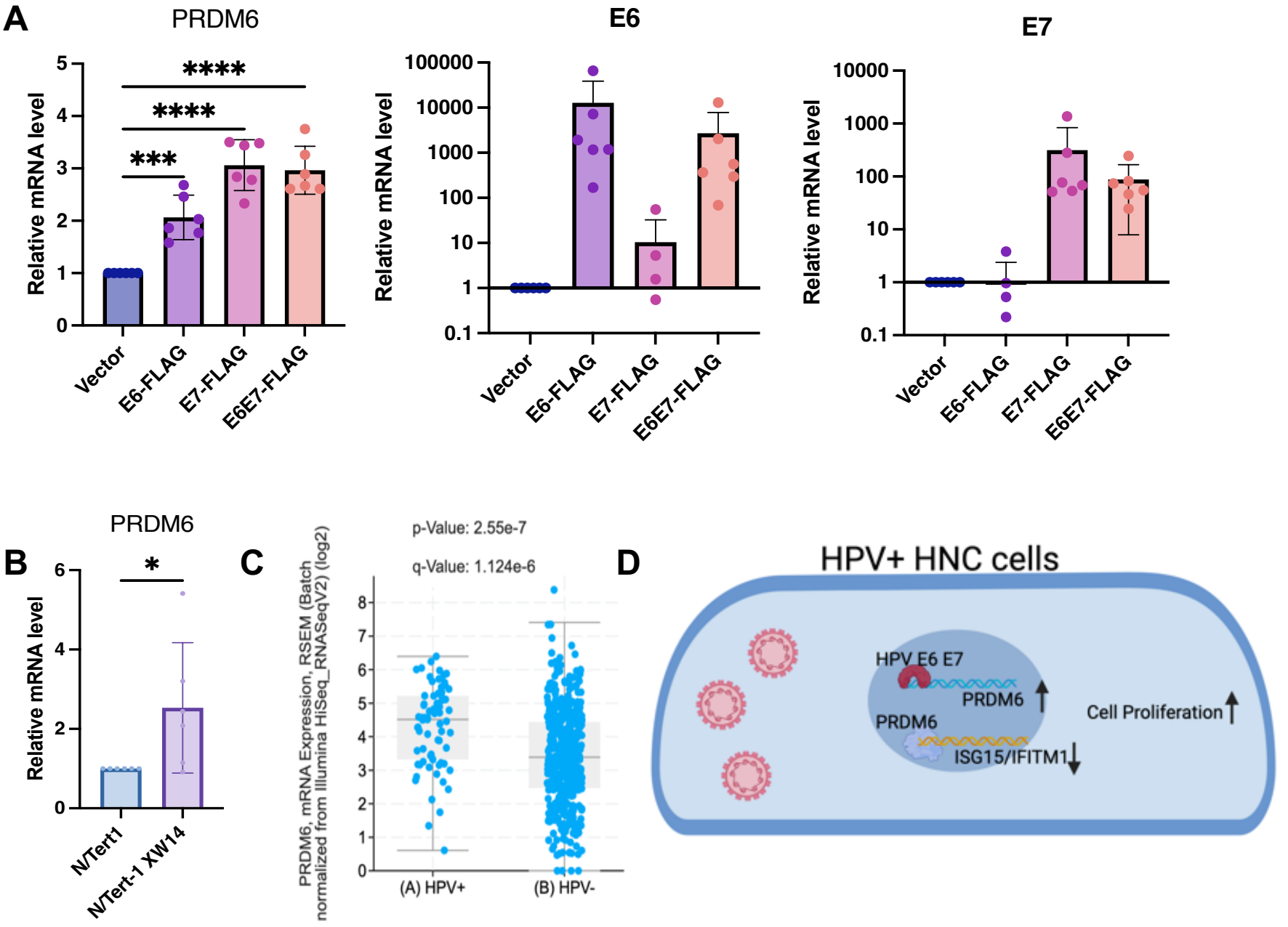
A
PRDM6
Relative mRNA level
****
****
***
Vector
E6-FLAG
E7-FLAG
E6E7-FLAG
E6
E7
B
PRDM6
*
N/Tert1
N/Tert-1 XW14
C
p-Value: 2.55e-7
q-Value: 1.124e-6
PRDM6, mRNA Expression, RSEM (Batch normalized from Illumina HiSeq_RNASeqV2) (log2)
(A) HPV+
(B) HPV-
D
HPV+ HNC cells
HPV E6 E7
PRDM6
PRDM6
ISG15/IFITM1
Cell Proliferation

Figure S1

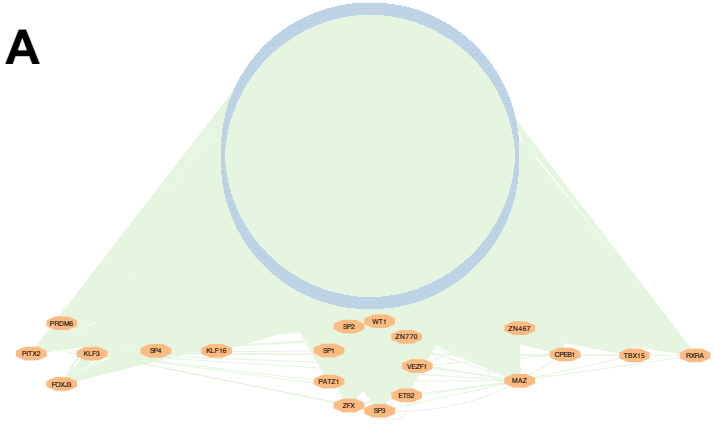
A
PRDM6
PITX2
KLF3
SP4
KLF16
SP2
WT1
SP1
ZN770
ZN467
CPEB1
TBX15
RXRA
VEZF1
MAZ
FOXJ3
PATZ1
ZFX
ETS2
SP3

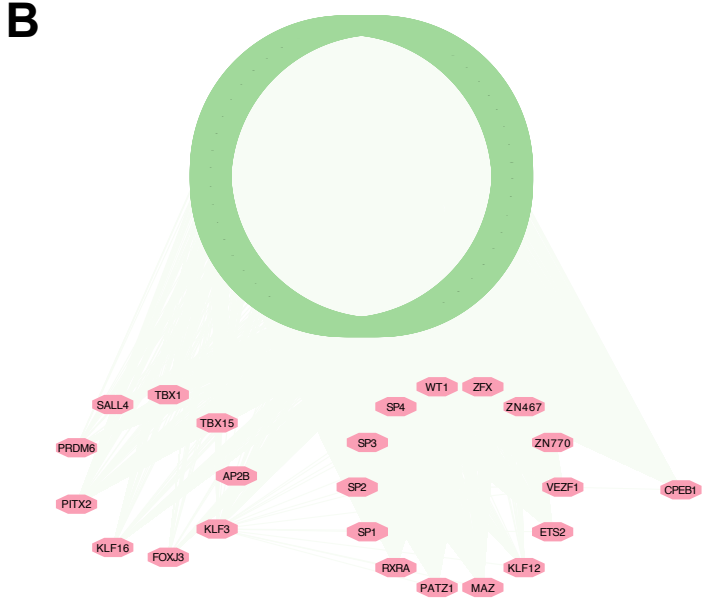
B
SALL4
TBX1
TBX15
PRDM6
PITX2
KLF16
AP2B
KLF3
FOXJ3
SP2
SP1
SP3
WT1
ZFX
SP4
ZN467
ZN770
VEZF1
CPEB1
ETS2
RXRA
KLF12
PATZ1
MAZ

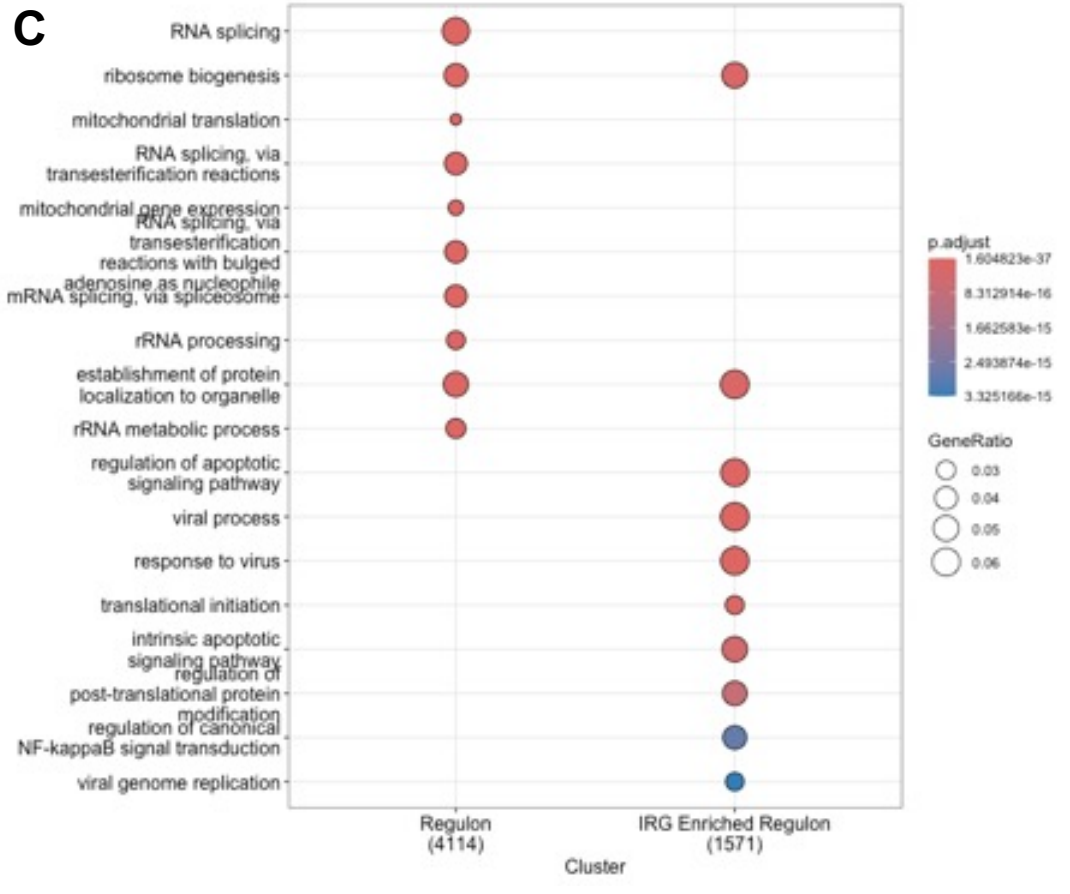
C
RNA splicing
ribosome biogenesis
mitochondrial translation
RNA splicing, via transesterification reactions
mitochondrial gene expression
RNA splicing, via transesterification reactions with bulged adenosine as nucleophile
mRNA splicing, via spliceosome
rRNA processing
establishment of protein localization to organelle
rRNA metabolic process
regulation of apoptotic signaling pathway
viral process
response to virus
translational initiation
intrinsic apoptotic signaling pathway
regulation of post-translational protein modification
regulation of canonical NF-kappaB signal transduction
viral genome replication
Regulon (4114)
IRG Enriched Regulon (1571)
Cluster
p.adjust
1.604823e-37
8.312914e-16
1.662583e-15
2.493874e-15
3.325166e-15
GeneRatio
0.03
0.04
0.05
0.06

Figure S2

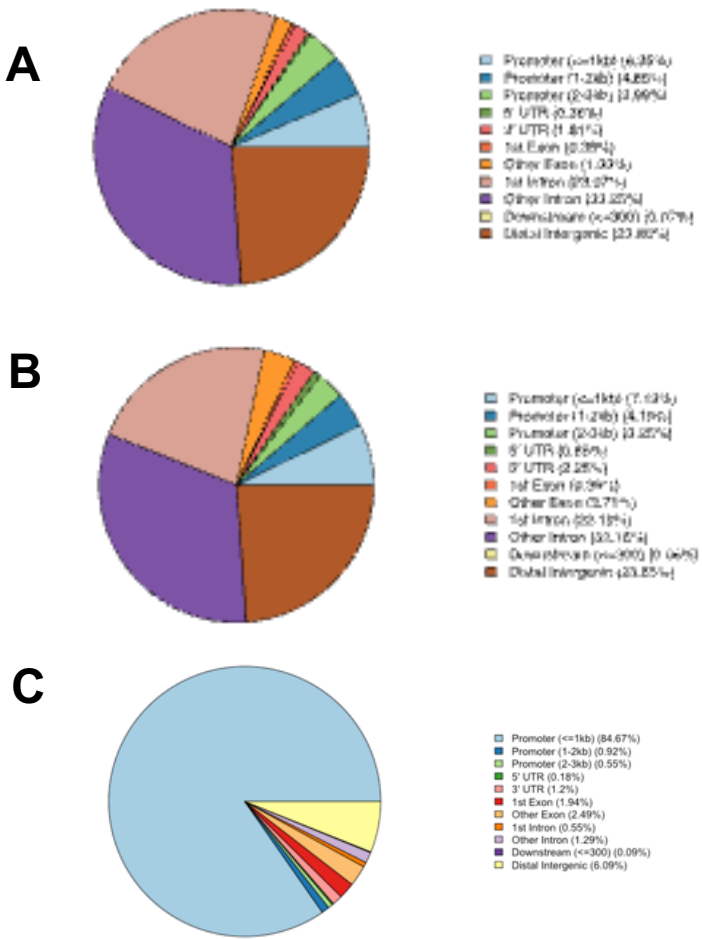
A
B
C
Promoter (<=1kb) (84.67%)
Promoter (1-2kb) (0.92%)
Promoter (2-3kb) (0.55%)
5' UTR (0.18%)
3' UTR (1.2%)
1st Exon (1.94%)
Other Exon (2.49%)
1st Intron (0.55%)
Other Intron (1.29%)
Downstream (<=300) (0.09%)
Distal Intergenic (6.09%)

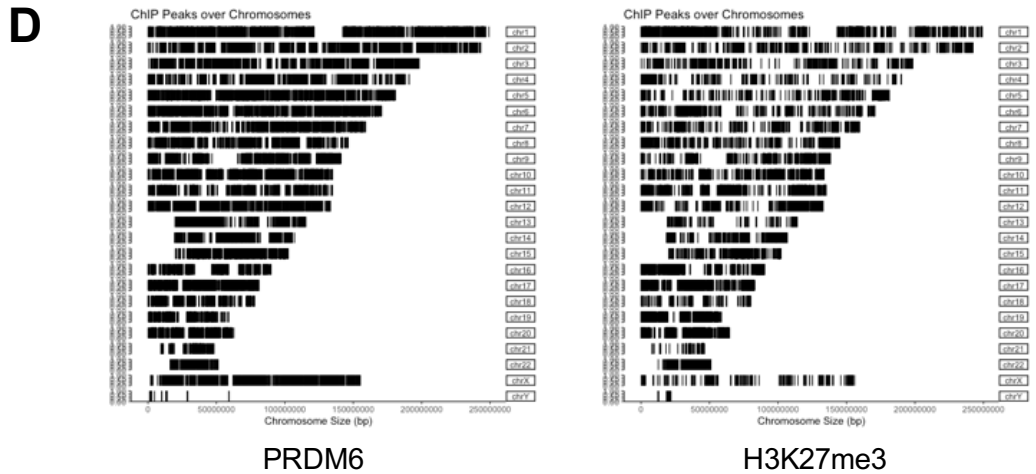
D
ChIP Peaks over Chromosomes
Chromosome Size (bp)
PRDM6
ChIP Peaks over Chromosomes
Chromosome Size (bp)
H3K27me3

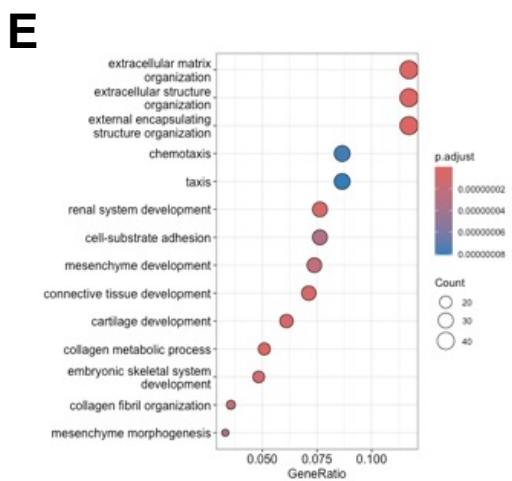
E
extracellular matrix organization
extracellular structure organization
external encapsulating structure organization
chemotaxis
taxis
renal system development
cell-substrate adhesion
mesenchyme development
connective tissue development
cartilage development
collagen metabolic process
embryonic skeletal system development
collagen fibril organization
mesenchyme morphogenesis
0.050
0.075
0.100
GeneRatio
p.adjust
Count

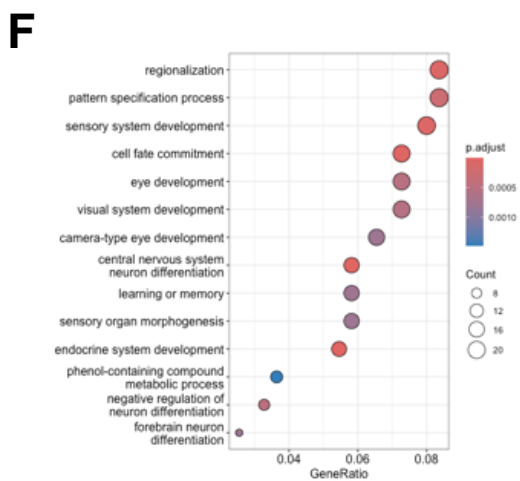
F
regionalization
pattern specification process
sensory system development
cell fate commitment
eye development
visual system development
camera-type eye development
central nervous system neuron differentiation
learning or memory
sensory organ morphogenesis
endocrine system development
phenol-containing compound metabolic process
negative regulation of neuron differentiation
forebrain neuron differentiation
0.04
0.06
0.08
GeneRatio
p.adjust
Count

Figure S3

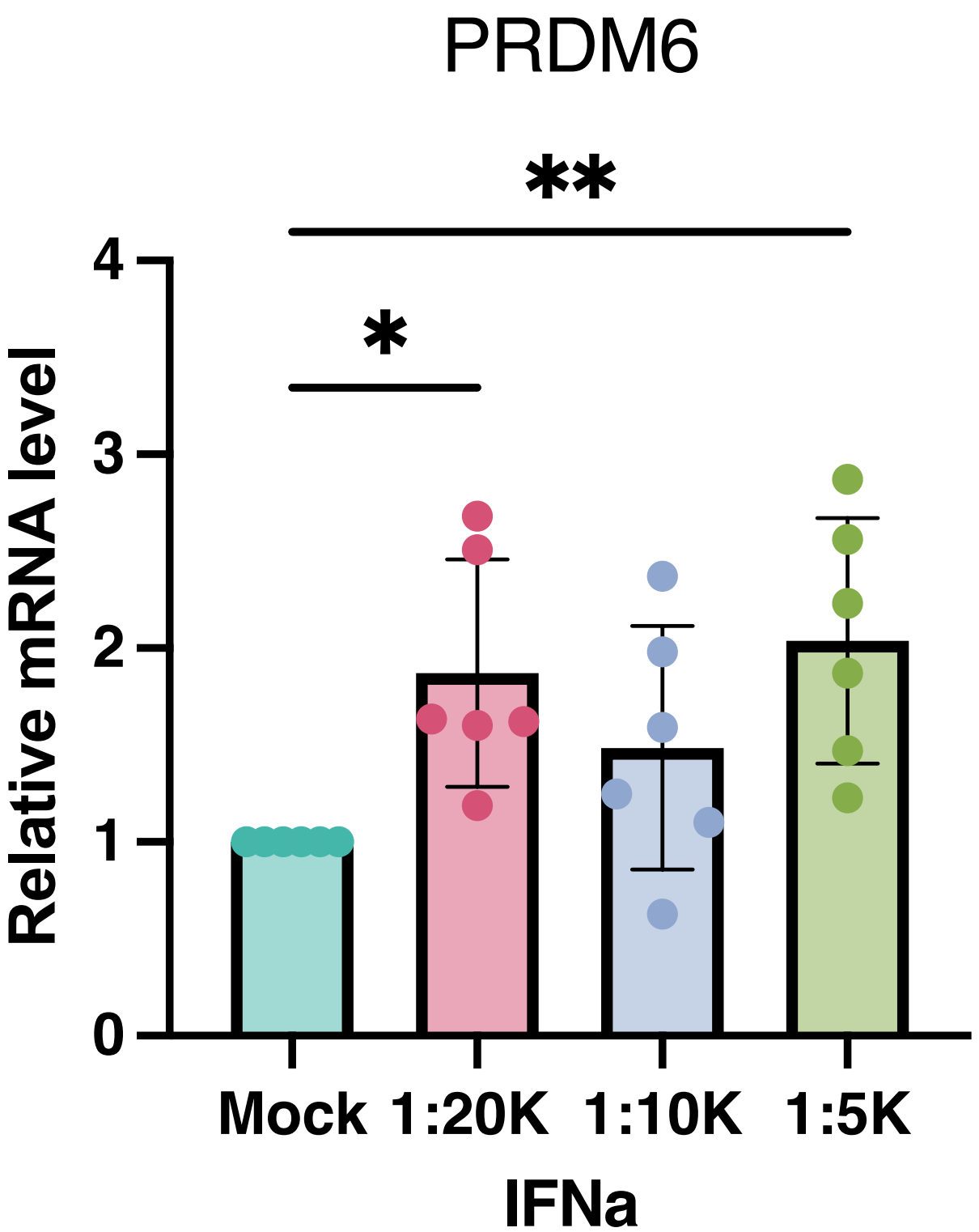

Figure S4

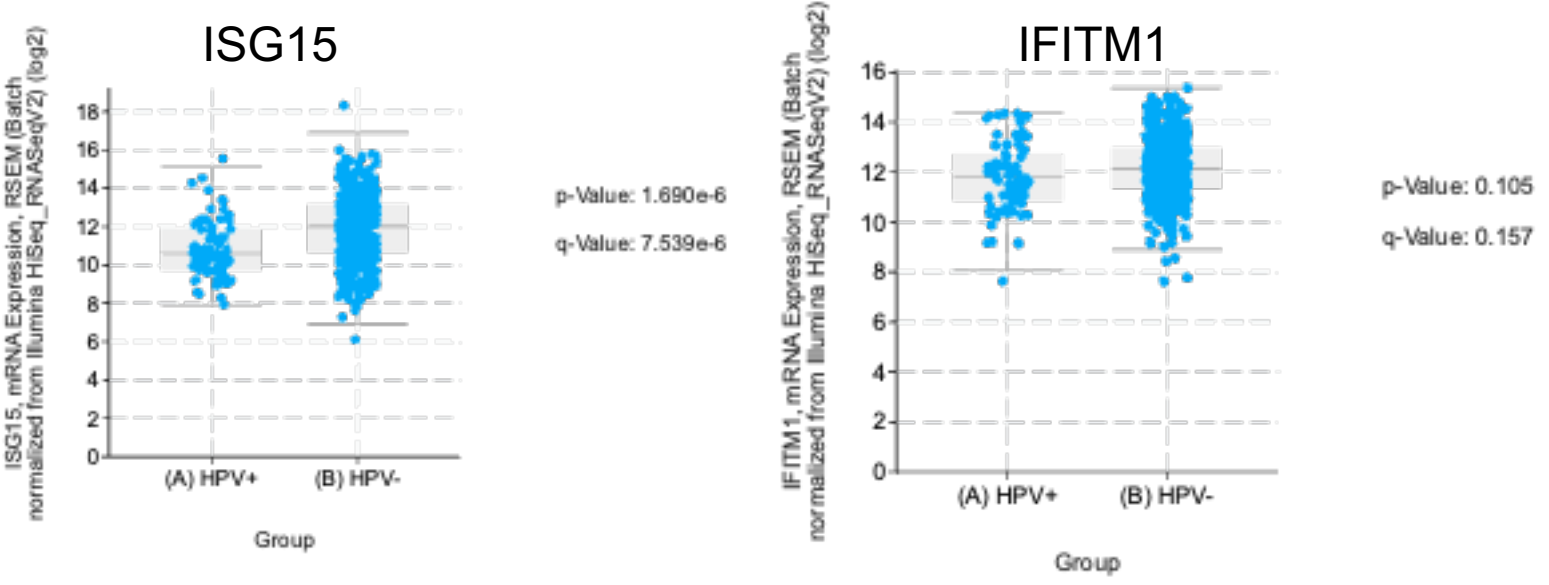
ISG15
ISG15, mRNA Expression, RSEM (Batch normalized from Illumina HiSeq_RNASeqV2) (log2)
18
16
14
12
10
8
6
4
2
0
(A) HPV+
(B) HPV-
Group
p-Value: 1.690e-6
q-Value: 7.539e-6
IFITM1
IFITM1, mRNA Expression, RSEM (Batch normalized from Illumina HiSeq_RNASeqV2) (log2)
16
14
12
10
8
6
4
2
0
(A) HPV+
(B) HPV-
Group
p-Value: 0.105
q-Value: 0.157

Table S1

tf_name	rss	rss_pval	gene_symbol	gene_id	Genenumb	hypogem_tes	hypogem_test_
TBX15	0.86541094	0	BCL11A,BCL	ENSG000001	215	0.44765376	0.66949824
TAF1	0.86417172	0	BCL11A,BCL	ENSG000001	112	0.31810053	0.61915009
E2F6	0.86372445	0	BCL7A,C6orf	ENSG000001	144	0.30703626	0.61915009
KLF12	0.86320489	0	BCL11A,BCL	ENSG000001	318	0.23418515	0.61592723
ETS2	0.86191172	0	ANKRD65,BC	ENSG000002	382	0.48156891	0.66949824
KLF6	0.86170654	0	ARHGAP29,B	ENSG000001	358	0.35157902	0.61915009
FLI1	0.86045429	0	BCL7A,C6orf	ENSG000001	153	0.1524828	0.51126585
RXRA	0.85971556	0	ANKRD65,AR	ENSG000002	632	0.2150655	0.61592723
WT1	0.85892039	0	BCL11A,BCL	ENSG000001	579	0.12175725	0.47823775
SP4	0.85829465	0	BCL11A,BCL	ENSG000001	336	0.73249295	0.78777543
KLF3	0.85741566	0	BCL11A,BCL	ENSG000001	365	0.71775861	0.78777543
ZF64A	0.85726416	0	BCL11A,BCL	ENSG000001	365	0.48043598	0.66949824
VEZF1	0.8571388	0	ANKRD65,AR	ENSG000002	672	0.39470213	0.64280061
MAZ	0.8559237	0	BCL11A,BCL	ENSG000001	659	0.13424217	0.47823775
PRDM6	0.8554473	0	BCL7A,C6orf	ENSG000001	133	0.84269875	0.85774694
PATZ1	0.85514827	0	ANKRD65,BC	ENSG000002	744	0.27301025	0.61592723
ZN467	0.85335418	0	ANKRD65,BC	ENSG000002	282	0.55651067	0.71314255
SP1	0.85329257	0	ANKRD65,AR	ENSG000002	861	0.0204371	0.20325987
ZFX	0.85327205	0	BCL11A,BCL	ENSG000001	645	0.03659783	0.29801089
SP3	0.85039609	0	ANKRD65,AR	ENSG000002	857	0.12323919	0.47823775
SP2	0.84974609	0	ANKRD65,AR	ENSG000002	899	0.06243617	0.39542907
CPEB1	0.84870964	0	BCL7A,C6orf	ENSG000001	557	0.27115674	0.61592723
KLF5	0.84792831	0	C6orf141,CK	ENSG000001	107	0.11754109	0.47823775
AP2D	0.8478074	0	BCL11A,CALI	ENSG000001	134	0.66366909	0.77202322
AP2B	0.84657099	0	C6orf141,CD	ENSG000001	101	0.4314807	0.66471352
ZN263	0.84482349	0	BCL11A,BCL	ENSG000001	295	0.24992625	0.61592723
ZN770	0.84393793	0	ANKRD65,AR	ENSG000002	1134	0.00076458	0.04358082
PITX2	0.84096443	0	BCL7A,C6orf	ENSG000001	278	0.71953191	0.78777543
PAX5	0.8351468	0	BCL11A,BCL	ENSG000001	79	0.7968256	0.82580108
KLF16	0.83439315	0	CKAP4,CLDN	ENSG000001	71	0.40950887	0.64838904
KLF15	0.83198139	0	BCL11A,BCL	ENSG000001	49	0.63071461	0.7489736
ZN219	0.82983776	0	BCL7A,CKAP	ENSG000001	51	0.88169454	0.88169454
THAP1	0.8199099	0	CLDN7,DSP,I	ENSG000001	21	0.57551855	0.71314255
ZBT17	0.81918514	0	ISYNA1,KREM	ENSG000001	20	0.32738625	0.61915009
NFAC1	0.79778534	0	CKAP4,EPCA	ENSG000001	11	0.50115515	0.68013914
ZN341	0.79373891	0	CALD1,CKAP	ENSG000001	40	0.0063423	0.18075563
FOXJ3	0.78690843	0	EPCAM,IGFB	ENSG000001	15	0.72446087	0.78777543
AP2C	0.77244687	0	CLDN7,BRI3	ENSG000001	19	0.28094926	0.61592723
HXC10	0.76788214	0	EPCAM,HOO	ENSG000001	13	0.3693176	0.61915009
KLF14	0.76065632	0	KRT18,S100A	ENSG000001	25	0.01966277	0.20325987
SPIB	0.75728974	0	EPCAM,ATN1	ENSG000001	11	0.24925968	0.61592723
ANDR	0.75643267	0	BCL7A,CALD	ENSG000001	15	0.04267384	0.30405109
TEAD2	0.74327056	0	S100A16,AC/	ENSG000001	36	0.77988385	0.82321073

BCL6	0.73906492	0	ACAT2,AFG3I	ENSG000001	13	0.3693176	0.61915009
NFAC2	0.73601498	0	ACBD3,ECE2	ENSG000001	8	0.59747598	0.72459852
ZN121	0.7290999	0	ACAT2,AFG3I	ENSG000001	21	0.57551855	0.71314255
ASCL1	0.72530204	0	ACAT2,AFG3I	ENSG000001	19	0.47762241	0.66949824
KLF1	0.72444826	0	AFG3L2,ARFI	ENSG000001	17	0.19381561	0.61374945
E2F3	0.72071073	0	ARFRP1,BRI3	ENSG000001	12	0.13030561	0.47823775
NRF1	0.71549833	0	CD27-AS1,CI	ENSG000002	7	0.5199215	0.68919826
MYOD1	0.71415761	0	CKAP4,CNN3	ENSG000001	5	0.33796404	0.61915009
ZBTB6	0.71221201	0	AFG3L2,ANKI	ENSG000001	14	0.21891339	0.61592723
STAT1	0.70552116	0	IGFBP2,IRF6,	ENSG000001	7	0.00995249	0.18909736
ARNT2	0.70043045	0	BRI3BP,IFRD	ENSG000001	8	0.02139578	0.20325987
SPDEF	0.69904678	0	BMS1,EXOSC	ENSG000001	5	0.33796404	0.61915009
MYCN	0.68606636	0	AFG3L2,ARFI	ENSG000001	11	0.09354659	0.47823775
ZN563	0.66622734	0.0174	ANKRD39,AP	ENSG000002	11	0.09354659	0.47823775
GFI1	0.54777409	0	CD151,FXYD	ENSG000001	8	0.59747598	0.597475976
EGR4	0.49187616	0	AAMP,ARFGA	ENSG000001	19	0.47762241	0.573146898
TBX15	0.48059316	0.0152	C1orf122,CC	ENSG000001	29	0.00966591	0.028997743
SOX2	0.47815428	0.0228	CKS1B,COMI	ENSG000001	12	0.13030561	0.260611229
STF1	0.47381908	0.0304	ALKBH7,GSN	ENSG000001	5	0.33796404	0.506946054
ZN341	0.46674629	0.038	DSP,AAMP,AI	ENSG000000	54	0.00157012	0.009420691
ZBT17	0.60910142	0	FXYD3,KRT18	ENSG000000	14	0.42947929	0.429479286
IRF3	0.5749614	0	AK3,CSTA,KR	ENSG000001	11	0.09354659	0.108207104
RARA	0.57016751	0	PERP,CD59,(	ENSG000001	9	0.14075318	0.149550256
MYNN	0.55071964	0	CSTA,MLF2,N	ENSG000001	8	0.09547686	0.108207104
ZN467	0.53220322	0	FXYD3,KRT18	ENSG000000	30	0.03376953	0.044160161
SP4	0.49137012	0.0138	ACADVL,AHN	ENSG000000	87	8.82E-10	1.50E-09
VEZF1	0.49126765	0.0138	CALML3,DSP	ENSG000001	171	2.86E-12	8.12E-12
TBX15	0.49090871	0.0138	ACADVL,AHC	ENSG000000	172	2.90E-10	5.53E-10
SP3	0.4773619	0.0184	FXYD3,PERP,	ENSG000000	518	3.88E-21	1.65E-20
PATZ1	0.47649311	0.0184	ACADVL,ACA	ENSG000000	193	2.93E-10	5.53E-10
ZN281	0.47383226	0.023	FXYD3,MIR2(	ENSG000000	49	0.00084657	0.00119931
ZN770	0.47157229	0.023	FXYD3,MIR2(	ENSG000000	688	2.21E-32	3.76E-31
RARB	0.4696986	0.023	KRT18,CCT2,	ENSG000001	28	1.16E-07	1.79E-07
MAZ	0.46615993	0.0276	ACADVL,ADH	ENSG000000	329	4.12E-14	1.40E-13
ZFX	0.4653111	0.0322	ACADVL,ACA	ENSG000000	229	1.50E-11	3.64E-11
SP1	0.465262	0.0322	AAMP,ACADV	ENSG000001	504	5.69E-29	4.83E-28
SP2	0.46472557	0.0322	AAK1,AAMP,A	ENSG000001	362	4.24E-25	2.40E-24
FLI1	0.81182136	0	ARHGAP29,B	ENSG000001	43	0.58088432	0.580884323
SALL4	0.80116985	0	ARHGAP29,B	ENSG000001	55	0.01102545	0.020310048
ZN263	0.80053605	0	ACKR3,BCAM	ENSG000001	67	0.09153379	0.125928101
AP2D	0.79992518	0	ARHGAP29,B	ENSG000001	68	0.10414539	0.135003277
ZN341	0.79941084	0	ARHGAP29,B	ENSG000001	36	0.33688006	0.368462566
KLF6	0.79223453	0	BCAM,GNG1	ENSG000001	97	0.0004459	0.001950793
SMAD1	0.79136007	0	ARHGAP29,B	ENSG000001	57	0.03353476	0.055891271
VDR	0.78475681	0	GNG12,IRF6,	ENSG000001	20	0.00913461	0.017761743

WT1	0.78316518	0	ACKR3,ARHG	ENSG000001	248	0.02778811	0.04862919
SP1	0.78163327	0	ACKR3,ARHG	ENSG000001	394	0.00586339	0.013681254
E2F6	0.78103789	0	BCAM,GNG1	ENSG000001	86	0.28340283	0.319970934
MAZ	0.77847886	0	ACKR3,ARHG	ENSG000001	388	0.00078949	0.003070228
KLF12	0.77807106	0	ACKR3,BCAM	ENSG000001	152	0.0520752	0.079244864
ZFX	0.7779924	0	ACKR3,ARHG	ENSG000001	447	1.11E-05	9.74E-05
VEZF1	0.77788979	0	ACKR3,ARHG	ENSG000001	369	0.00111674	0.003553277
AP2B	0.7758909	0	GNG12,IRF6,	ENSG000001	28	0.04703543	0.074829094
SP4	0.77486955	0	BCAM,IRF6,I	ENSG000001	68	0.0009757	0.003414959
KLF3	0.77369258	0	BCAM,GNG1	ENSG000001	179	0.00273797	0.006844921
KLF16	0.77260485	0	IRF6,ITGA2,N	ENSG000001	38	0.00035863	0.001793143
PATZ1	0.77152362	0	ACKR3,ARHG	ENSG000001	531	4.89E-06	5.70E-05
RXRA	0.77145389	0	BCAM,IRF6,N	ENSG000001	57	0.00814953	0.016778451
E2F7	0.77058072	0	ARHGAP29,G	ENSG000001	22	0.24822179	0.289592091
PITX2	0.76995409	0.0052	ACKR3,ARHG	ENSG000001	213	0.00809224	0.016778451
SP3	0.76780917	0.0052	ACKR3,ARHG	ENSG000001	611	7.50E-05	0.000437233
THA	0.76563452	0.0052	IRF6,KRTCAP	ENSG000001	33	0.00157582	0.004242582
TBX15	0.76470908	0.0052	BCAM,GNG1	ENSG000001	192	0.00136677	0.00398642
BHA15	0.76424705	0.0104	ARHGAP29,B	ENSG000001	24	0.51475237	0.545949489
IRF3	0.76394495	0.0104	ARHGAP29,G	ENSG000001	14	0.21891339	0.26420581
PLAL1	0.76384606	0.0104	ITGA2,KCTD1	ENSG000001	12	0.56529463	0.580884323
SP2	0.76330725	0.0104	ACKR3,ARHG	ENSG000001	595	1.54E-09	5.38E-08
ZN770	0.76308741	0.0104	ACKR3,ARHG	ENSG000001	734	7.72E-09	1.35E-07
ANDR	0.76302842	0.0104	ARHGAP29,IF	ENSG000001	11	0.09354659	0.125928101
CPEB1	0.76230571	0.0104	ACKR3,ARHG	ENSG000001	359	6.00E-05	0.000420257
ESR2	0.75405481	0.0416	BCAM,GNG1	ENSG000001	10	0.06292785	0.091769778
ETV5	0.75325132	0.0468	IRF6,NAV2,PI	ENSG000001	10	0.19263674	0.240795923
ZN219	0.81593887	0	CACNA2D1,C	ENSG000001	95	0.75783495	0.814672576
RXRA	0.81449366	0	CALML3,CDC	ENSG000001	92	0.24380499	0.388282026
ZN281	0.81147215	0	CALML3,GPX	ENSG000001	33	0.69225798	0.7632588
SALL4	0.80924021	0	CALML3,GPX	ENSG000001	37	0.80456207	0.843809005
E2F6	0.80837774	0	CACNA2D1,C	ENSG000001	140	0.10091696	0.188670847
KLF15	0.80748965	0	CACNA2D1,C	ENSG000001	118	0.354988	0.508816132
KLF8	0.80696015	0	CALML3,GPX	ENSG000001	26	0.60106739	0.738454223
EGR2	0.8057927	0	CALML3,EGF	ENSG000001	31	0.62264218	0.743711494
PRDM6	0.80502202	0	CALML3,EGF	ENSG000001	73	0.67741183	0.7632588
SP4	0.80319622	0	CACNA2D1,C	ENSG000001	111	0.37961675	0.526565167
ZN467	0.80309355	0	CACNA2D1,C	ENSG000001	164	0.03812292	0.091071427
ZN341	0.80214885	0	CACNA2D1,C	ENSG000001	179	0.17692836	0.316996648
ZN257	0.79807083	0	GPX2,ITGA2,I	ENSG000001	19	0.68967532	0.7632588
KLF1	0.79523625	0	EGFR,GPX2,I	ENSG000001	30	0.0753654	0.154319628
EGR4	0.79446876	0	CALML3,CDC	ENSG000001	30	0.03376953	0.085417059
IRF3	0.79214063	0	CALML3,IRF6	ENSG000001	17	0.93588103	0.935881029
TBX15	0.79111114	0	CACNA2D1,C	ENSG000001	172	0.07963891	0.155657861
KLF6	0.78863449	0	CALML3,GPX	ENSG000001	17	0.59632898	0.738454223

ZN263	0.78749875	0	CALML3,CDC	ENSG000001	149	0.0562945	0.124106495
KLF12	0.78519014	0	CALML3,EMP	ENSG000001	80	0.42740465	0.574325004
KLF5	0.78345153	0	CACNA2D1,C	ENSG000001	100	0.011929	0.034196462
VEZF1	0.7804691	0	CACNA2D1,C	ENSG000001	311	0.00053567	0.001771845
MAFG	0.78029065	0	EGFR,GPX2,I	ENSG000001	19	0.05772395	0.124106495
ZBT17	0.77874376	0	CALML3,GPX	ENSG000001	13	0.84880103	0.869010579
AP2B	0.77786242	0	CACNA2D1,C	ENSG000001	273	0.02384502	0.064083492
ZN148	0.7743692	0	KRTCAP3,NTI	ENSG000001	7	0.21534011	0.356139407
ZN121	0.7739081	0	CACNA2D1,C	ENSG000001	74	0.2012034	0.34606985
ZFX	0.77358063	0	CACNA2D1,C	ENSG000001	395	0.00014491	0.000623092
WT1	0.77028389	0	CACNA2D1,C	ENSG000001	542	4.94E-06	3.04E-05
MAZ	0.76738903	0	CACNA2D1,C	ENSG000001	479	0.0001355	0.000623092
FLI1	0.76692503	0	CALML3,CDC	ENSG000001	245	5.37E-05	0.000288871
ETS2	0.76597448	0	CALML3,CDC	ENSG000001	397	0.0054705	0.016802246
TBX1	0.76018373	0	CALML3,GPX	ENSG000001	8	0.28725806	0.4411463
TAF1	0.75877527	0	CACNA2D1,C	ENSG000001	461	0.00021321	0.000833476
PATZ1	0.75514006	0	CACNA2D1,C	ENSG000001	577	1.61E-07	1.16E-06
SP2	0.75354136	0	CACNA2D1,C	ENSG000001	697	1.15E-07	9.89E-07
KLF16	0.75245094	0	CALML3,GPX	ENSG000001	39	0.59313879	0.738454223
ETV2	0.75240799	0	ITGA2,PRRX1	ENSG000001	5	0.33796404	0.501119088
SP3	0.75159811	0	CACNA2D1,C	ENSG000001	857	7.60E-09	1.63E-07
SP1	0.75135934	0	CACNA2D1,C	ENSG000001	655	5.38E-08	7.72E-07
CPEB1	0.74196491	0	EGFR,EMP2,I	ENSG000001	455	7.33E-08	7.88E-07
ZN770	0.74172148	0	CACNA2D1,C	ENSG000001	973	4.68E-10	2.01E-08
PITX2	0.72662561	0	FERMT1,IRF6	ENSG000001	153	0.00038596	0.001383022
TBX15	0.84751617	0	ABCA13,CNN	ENSG000001	83	0.04038744	0.0793822
RARB	0.8472232	0	ABCA13,CNN	ENSG000001	74	0.05279686	0.100314034
SALL4	0.8407455	0	CNN3,CP,CF	ENSG000001	65	0.11416011	0.158710403
SMAD4	0.84056506	0	ABCA13,CNN	ENSG000001	34	0.1584873	0.192208003
E2F7	0.83958868	0	ABCA13,CNN	ENSG000001	93	0.00080696	0.00270331
ZN263	0.83787953	0	ABCA13,CNN	ENSG000001	82	0.14112139	0.187067882
SRBP2	0.83763186	0	ABCA13,CNN	ENSG000001	83	0.06642248	0.111355332
ZN281	0.83586187	0	ABCA13,CNN	ENSG000001	70	0.08352303	0.132244799
ZF64A	0.83574167	0	ABCA13,CNN	ENSG000001	70	0.08352303	0.132244799
PRDM6	0.83458802	0	ABCA13,CRC	ENSG000001	85	0.35026807	0.383947692
TBX1	0.83389411	0	ABCA13,CNN	ENSG000001	46	0.27783118	0.314002119
VEZF1	0.83315284	0	ABCA13,CNN	ENSG000001	198	0.00022202	0.001054582
KLF3	0.83270103	0	CNN3,CROT	ENSG000001	76	0.11080162	0.158710403
ZN467	0.83090675	0	ABCA13,CNN	ENSG000001	188	0.00351999	0.010031977
CTCFL	0.83052195	0	CNN3,CROT	ENSG000001	36	0.06273017	0.108352114
NR1I3	0.8299856	0	ABCA13,CNN	ENSG000001	24	0.01392881	0.034519224
ETS2	0.82904834	0	ABCA13,CNN	ENSG000001	119	0.00035773	0.001359381
FOXJ3	0.82866104	0	ABCA13,FAB	ENSG000001	20	0.1725963	0.204958109
ZN341	0.82753963	0	ABCA13,CNN	ENSG000001	203	0.00085368	0.00270331
AP2D	0.8274033	0	ABCA13,CNN	ENSG000001	197	0.00168156	0.005044671

ETV2	0.8240546	0	ABCA13,CNN	ENSG000001	25	0.11324392	0.158710403
E2F6	0.82395816	0	CNN3,CROT	ENSG000001	38	0.02131271	0.048592987
PITX2	0.82249916	0	FABP6,FBLN	ENSG000001	34	0.1584873	0.192208003
KLF5	0.82181686	0	ABCA13,IRF6	ENSG000001	17	0.37316991	0.388032898
MAZ	0.82146412	0	CNN3,CROT	ENSG000001	198	0.00022202	0.001054582
SUH	0.82071781	0	CROT,FABP6	ENSG00000C	43	0.03165321	0.066823438
ZBT17	0.81928143	0	ABCA13,FBLI	ENSG000001	18	0.6450326	0.6450326
EGR2	0.81928011	0	CNN3,FBLN1	ENSG000001	24	0.18622594	0.216630173
KLF6	0.8184042	0	CNN3,FZD6,	ENSG000001	16	0.06080204	0.108303631
RFX1	0.81780847	0	ABCA13,CNN	ENSG000001	237	0.00024171	0.001059784
KLF12	0.8169478	0	ABCA13,CNN	ENSG000001	188	0.00074488	0.002653622
KLF1	0.81682126	0	CNN3,FBLN1	ENSG000001	16	0.06080204	0.108303631
FUBP1	0.81663782	0	ABCA13,FBLI	ENSG000001	11	0.09354659	0.140319884
NKX25	0.8150516	0	FBLN1,IRF6,I	ENSG00000C	14	0.02843762	0.062344015
ZN219	0.81322106	0	CNN3,IRF6,K	ENSG000001	15	0.11948264	0.16215501
TAF1	0.81159448	0	ABCA13,CNN	ENSG000001	301	3.25E-06	2.06E-05
FLI1	0.80682662	0	ABCA13,CNN	ENSG000001	29	0.37441771	0.388032898
RXRA	0.80680866	0	ABCA13,CNN	ENSG000001	492	0.00035434	0.001359381
SP1	0.80238265	0	ABCA13,CNN	ENSG000001	498	8.51E-08	6.93E-07
SP4	0.80180356	0	CNN3,CROT	ENSG000001	145	7.72E-05	0.000439958
CPEB1	0.800398	0	ABCA13,CNN	ENSG000001	455	1.30E-08	1.49E-07
WT1	0.80016658	0	ABCA13,CNN	ENSG000001	579	1.39E-06	9.92E-06
SP2	0.79984465	0	ABCA13,CNN	ENSG000001	690	5.19E-10	7.39E-09
ZFX	0.79757553	0	ABCA13,CNN	ENSG000001	662	1.99E-08	1.89E-07
SP3	0.79628347	0	ABCA13,CNN	ENSG000001	747	2.23E-11	4.24E-10
KLF16	0.79453609	0	CNN3,IRF6,K	ENSG000001	19	0.28094926	0.314002119
PATZ1	0.79452021	0	ABCA13,CNN	ENSG000001	710	1.47E-13	4.18E-12
ZN770	0.79175852	0	ABCA13,CNN	ENSG000001	899	3.29E-14	1.88E-12
AP2B	0.79112562	0	CROT,KIAA12	ENSG00000C	14	0.42947929	0.437148559
NRF1	0.78794165	0	FBLN1,MPZL1	ENSG00000C	11	0.09354659	0.140319884
TEAD1	0.7873881	0	FBLN1,PTGES	ENSG00000C	19	0.02001109	0.047526333
NFKB2	0.78554921	0	FZD6,KRT18,	ENSG000001	6	0.14809562	0.187587792
IRF3	0.7846248	0	FABP6,IRF6,N	ENSG000001	148	0.00538648	0.01462044
ZSC22	0.78260616	0	ABCA13,FBLI	ENSG000001	9	0.03888145	0.079151523
MYNN	0.76314754	0	KRT18,CCND	ENSG000001	9	0.36051049	0.387718832
ZN148	0.75461491	0	KRT18,S100A	ENSG000001	6	0.14809562	0.187587792
MAFA	0.73661881	0.0057	FBLN1,BCL1	ENSG00000C	5	0.01259944	0.032643996
KLF6	0.5684869	0	CCND1,CNN	ENSG000001	32	0.65852468	0.706709409
ZF64A	0.56281355	0	CCND1,CNN	ENSG000001	25	0.73741505	0.77253005
ZN281	0.55378297	0	CCND1,CKA	ENSG000001	26	0.76987878	0.772740569
ZN467	0.51958543	0	CCND1,CKA	ENSG000001	119	0.03741725	0.082317941
ZN320	0.51310846	0	ATP1B1,CD9	ENSG000001	12	0.56529463	0.637768304
ZN528	0.50594006	0	ATP1B1,FXYD	ENSG000001	11	0.77274057	0.772740569
SOX4	0.49946253	0	CD9,FXYD3,(	ENSG00000C	8	0.09547686	0.162969667
ETV2	0.4989377	0	CD9,FXYD3,(	ENSG00000C	10	0.43245639	0.514272461

SRBP2	0.49347481	0	ATP1B1,CCN	ENSG000001	25	0.05061308	0.106046459
ZN341	0.48483307	0	CCND1,DSP	ENSG000001	60	0.09630026	0.162969667
ZN148	0.48128509	0	ACADVL,CD9	ENSG000000	9	0.14075318	0.206438
ZN257	0.4774963	0	AP1S1,BOLA3	ENSG000001	18	0.42586632	0.514272461
MAZ	0.47408137	0	CCND1,CHC	ENSG000001	202	0.00024252	0.000889254
FOXJ3	0.46808551	0	ALDH9A1,AN	ENSG000001	53	0.25493039	0.320483913
WT1	0.46466973	0	RCN1,AAMP,	ENSG000000	310	1.70E-09	1.07E-08
TBR1	0.46457995	0	CST3,CYTH2	ENSG000001	8	0.59747598	0.657223573
AP2B	0.46303769	0	BAD,CYB5A,I	ENSG000000	10	0.01483505	0.038396607
RARB	0.46292854	0	DSP,EMP2,M	ENSG000000	80	0.02555967	0.062479202
SP1	0.46255546	0	ALDH2,CCNI	ENSG000001	417	5.11E-10	4.50E-09
HMX2	0.46251201	0	EI24,FEZ2,KR	ENSG000001	7	0.5199215	0.602014364
FOXG1	0.46189037	0	CD9,KRT19,N	ENSG000000	5	0.08941345	0.162969667
KLF14	0.4617852	0	AP1S1,ARL2,I	ENSG000001	25	0.11324392	0.177954728
EGR1	0.4617852	0	AP1S1,ARL2,I	ENSG000001	25	0.11324392	0.177954728
KLF16	0.45844904	0.0079	CCND1,CAP	ENSG000001	57	0.00814953	0.022411217
ZN322	0.45423997	0.0079	ADD3,CD9,F	ENSG000001	7	0.21534011	0.287120142
ZFX	0.45230907	0.0079	ALDH2,CCNI	ENSG000001	604	6.89E-14	2.16E-12
SP3	0.45202578	0.0079	CCND1,CNN	ENSG000001	317	8.98E-10	6.59E-09
SP4	0.45083566	0.0079	CCND1,CNN	ENSG000001	214	0.00148316	0.004661353
KLF5	0.44725625	0.0079	ATP1B1,CD9	ENSG000001	9	0.14075318	0.206438
ETS2	0.44719579	0.0079	CCND1,CHC	ENSG000001	183	3.03E-06	1.21E-05
SP2	0.44670582	0.0079	CCND1,CNN	ENSG000001	424	7.67E-08	4.22E-07
PATZ1	0.44319379	0.0079	CCND1,CKA	ENSG000001	501	1.47E-13	2.16E-12
KLF12	0.44265976	0.0079	AP1S1,ARL2,I	ENSG000001	54	0.00383114	0.011238018
AP2D	0.43857458	0.0158	AAMP,ADAM1	ENSG000001	207	8.91E-07	3.92E-06
KLF3	0.43687819	0.0158	CCL19,CD9,(	ENSG000001	27	0.08266423	0.158140263
TBX15	0.43641453	0.0158	ACTR1B,AKR	ENSG000001	209	3.14E-07	1.54E-06
ZBTB4	0.43444749	0.0158	DHX29,EI24,I	ENSG000000	6	0.14809562	0.210200242
SMCA1	0.43121911	0.0158	BOLA3,CDK4	ENSG000001	11	0.24925968	0.320483913
RXRA	0.43099434	0.0158	CCND1,DSP	ENSG000001	280	4.16E-12	4.58E-11
TBX1	0.42813921	0.0237	ACO2,ADSL,A	ENSG000001	63	0.00140183	0.004661353
VEZF1	0.42809112	0.0237	CCND1,CKA	ENSG000001	351	1.02E-13	2.16E-12
NR1I3	0.42455791	0.0316	AP1S1,ARL2,I	ENSG000001	16	0.154691	0.212700124
TFEB	0.42359393	0.0316	ARL2,BOLA3,	ENSG000002	10	0.06292785	0.125855695
CTCFL	0.42291163	0.0316	AP1S1,BAD,B	ENSG000001	23	0.02810623	0.065088113
ZN341	0.85360872	0	CDK4,CLDN	ENSG000001	13	0.3693176	0.391366412
NFIC	0.83461001	0	CDK4,CLDN	ENSG000001	14	0.42947929	0.445446017
ZN331	0.83108413	0	CLDN1,KRT1	ENSG000001	9	0.6651804	0.674682977
ZN121	0.82457495	0	CDK4,CLDN	ENSG000001	26	0.06539308	0.081454533
PURA	0.81882437	0	FXYD3,KRT1	ENSG000000	7	0.8483062	0.848306199
PPARA	0.79348654	0	CDK4,KRT19	ENSG000001	5	0.33796404	0.363567372
ZN281	0.79332204	0	CDK4,CLDN	ENSG000001	39	4.74E-07	1.35E-06
VEZF1	0.78806288	0	CD24,CD9,C	ENSG000002	78	2.93E-05	6.30E-05
TFEB	0.78518536	0	CDK4,KRT19	ENSG000001	9	0.14075318	0.161185095

TBX1	0.78249127	0	CD24,CLDN	ENSG000002	31	0.0022506	0.003195851
SPIB	0.78070388	0	KRT18,KRT19	ENSG000001	6	0.14809562	0.164293584
MEF2B	0.77852835	0	EPCAM,GPNI	ENSG000001	13	0.01779034	0.023391008
RARB	0.77601221	0	CD24,CD9,C	ENSG000002	80	1.42E-09	6.30E-09
ZN467	0.77346386	0	CD24,CD9,C	ENSG000002	79	1.29E-08	4.35E-08
RREB1	0.7732441	0	CDK4,KRT19,	ENSG000001	5	0.08941345	0.107599236
ZN148	0.77320605	0	AHCY,CDK4,	ENSG000001	22	0.00038357	0.000605194
PRDM6	0.77165483	0	AHCY,CDK4,	ENSG000001	54	2.20E-05	4.92E-05
ANDR	0.76592747	0	CDK4,KRT18,	ENSG000001	19	4.35E-05	9.08E-05
EGR4	0.7592765	0	CDK4,KRT18,	ENSG000001	35	0.00032691	0.000527514
ETV5	0.75726576	0	CDK4,KRT5,K	ENSG000001	24	0.000275	0.000454064
ZN263	0.75136768	0	CDK4,KRT18,	ENSG000001	22	7.32E-05	0.000133255
KLF3	0.75077554	0	CDK4,PERP,S	ENSG000001	8	0.09547686	0.112980947
SP3	0.74995307	0	AHCY,CALML	ENSG000001	193	2.14E-13	2.17E-12
ZN219	0.74933589	0	AHCY,CDK4,	ENSG000001	65	1.80E-09	7.10E-09
HXD13	0.74839102	0	KRT18,KRT19	ENSG000001	33	6.05E-06	1.48E-05
WT1	0.74718518	0	AHCY,CD24,	ENSG000001	117	1.54E-12	1.21E-11
MAZ	0.74619811	0	CD24,CD9,C	ENSG000002	92	9.71E-09	3.45E-08
TBX15	0.74549802	0	CD24,CD9,C	ENSG000002	92	7.46E-10	3.92E-09
PATZ1	0.7430606	0	AHCY,ANXA8	ENSG000001	310	1.99E-18	3.53E-17
FOXL1	0.74059263	0	KRT18,KRT19	ENSG000001	6	0.43289824	0.445446017
SP4	0.73655491	0	AHCY,CD9,C	ENSG000001	84	7.32E-10	3.92E-09
TGIF1	0.72973174	0	CDK4,PERP,S	ENSG000001	7	0.21534011	0.235217655
HXC10	0.7292827	0	CDK4,PERP,S	ENSG000001	28	8.54E-07	2.25E-06
RXRA	0.72916734	0	CDK4,CLDN	ENSG000001	77	2.31E-07	6.84E-07
KLF15	0.72499141	0	AHCY,CDK4,	ENSG000001	199	1.63E-18	3.53E-17
SP2	0.71992895	0	AHCY,CD24,	ENSG000001	261	2.51E-25	8.89E-24
ZBT17	0.71786849	0	CDK4,SOX4,A	ENSG000001	18	0.0007391	0.001116513
AP2C	0.71751693	0	CDK4,KRT19,	ENSG000001	6	0.14809562	0.164293584
ZN586	0.71579339	0	CDK4,KRT18,	ENSG000001	14	0.02843762	0.036710384
ASCL1	0.7147168	0	AHCY,CDK4,	ENSG000001	192	2.78E-18	3.95E-17
ZFX	0.7146791	0	CDK4,FXYD3	ENSG000001	60	1.74E-12	1.24E-11
PITX2	0.71262795	0	AHCY,ANXA8	ENSG000001	187	7.74E-10	3.92E-09
FOXJ3	0.70870011	0	CDK4,ADH5,	ENSG000001	17	5.42E-05	0.000110015
TBX5	0.70826686	0	CDK4,ANAPC	ENSG000001	11	0.00078616	0.001162857
AP2B	0.70004074	0	CDK4,SOX4,A	ENSG000001	39	2.37E-06	6.00E-06
GATA3	0.69914431	0	SOX4,SPINT2	ENSG000001	9	0.03888145	0.049296124
THA	0.69897122	0	CDK4,ANAPC	ENSG000001	8	0.00025906	0.000437942
TEAD1	0.69805092	0	CDK4,ADH5,	ENSG000001	22	1.16E-05	2.76E-05
ZN770	0.69754111	0	AHCY,CD24,	ENSG000001	444	2.17E-26	1.54E-24
GATA4	0.69303515	0	AHCY,PERP,I	ENSG000001	5	0.01259944	0.016878491
CPEB1	0.69189439	0	AHCY,CD9,C	ENSG000001	237	1.17E-15	1.39E-14
FLI1	0.68935004	0	CDK4,ADH5,	ENSG000001	41	1.65E-09	6.90E-09
NFAC1	0.68643538	0	AKR1A1,ANAI	ENSG000001	16	0.00016406	0.000291206
ZSC22	0.68430745	0	AHCY,CDK4,	ENSG000001	64	1.95E-10	1.26E-09

E2F7	0.6837348	0	ACP1,ANAPC	ENSG000001	32	5.26E-07	1.44E-06
PAX5	0.68299514	0	KRT19,ACP1,	ENSG000001	47	8.36E-10	3.96E-09
ETS2	0.68273371	0	ACP1,AKR1A	ENSG000001	42	1.33E-07	4.10E-07
KLF6	0.68166014	0	ACP1,AKR1A	ENSG000001	25	4.66E-08	1.50E-07
KLF12	0.68161871	0	SGK1,ACAP2	ENSG000001	50	7.83E-09	2.92E-08
TFE3	0.68126072	0	CDK4,COA3,	ENSG000001	5	0.08941345	0.107599236
RXRB	0.67920437	0	CDK4,ANAPC	ENSG000001	7	0.00096593	0.001399611
SP1	0.67851315	0	AHCY,CD24,	ENSG000001	114	1.28E-12	1.14E-11
ITF2	0.67771726	0	ANAPC5,DUT	ENSG00000C	14	2.22E-05	4.92E-05
ESR2	0.6722931	0	ANAPC5,G3B	ENSG00000C	9	6.85E-05	0.000131378
RARA	0.67211241	0	AHCY,AK2,AN	ENSG000001	25	0.00048948	0.000755505
NRF1	0.66855822	0	CDK4,ANAPC	ENSG000001	22	7.32E-05	0.000133255
LYL1	0.66085262	0	SOX4,ANKRD	ENSG000001	9	0.14075318	0.161185095
THAP1	0.65663141	0	AKR1A1,EIF2	ENSG000001	9	6.85E-05	0.000131378
SALL4	0.65539899	0	CDK4,ACAP2	ENSG000001	26	0.00019676	0.000340737
KLF5	0.65206496	0	CDK4,ACP1,(	ENSG000001	10	0.00245536	0.003418246
ZN740	0.64563929	0	AKR1A1,EIF2	ENSG000001	7	0.00995249	0.01358898
ZBT17	0.81774383	0	CD9,CLDN1,	ENSG00000C	10	0.43245639	0.432456388
RARB	0.77020429	0	CD9,CSTA,D	ENSG00000C	22	0.00038357	0.000537003
PRDM6	0.76379691	0	CLDN1,CSTA	ENSG000001	31	0.0022506	0.002780152
FUBP1	0.75858772	0	CLDN1,DSP,I	ENSG000001	10	0.01483505	0.015976211
TBX15	0.75697914	0	CD9,CLDN1,	ENSG00000C	71	4.95E-08	9.91E-08
ZN341	0.75325689	0	CCND1,CD9	ENSG000001	108	1.84E-10	4.83E-10
SP4	0.75179482	0	CD9,CLDN1,	ENSG00000C	81	1.39E-12	4.87E-12
TBX1	0.75040145	0	CD9,KRT19,K	ENSG00000C	25	0.00193783	0.002466328
RXRA	0.74788312	0	CCND1,CD9	ENSG000001	131	2.40E-11	6.73E-11
VEZF1	0.74688429	0	CD9,CLDN1,	ENSG00000C	74	8.79E-12	2.83E-11
ETS2	0.74319632	0	ALDH1A1,CC	ENSG000001	301	6.11E-25	1.28E-23
SP1	0.74183992	0	CCND1,CD9	ENSG000001	232	1.17E-20	7.02E-20
ZN121	0.74139272	0	ABCC5,KRT1	ENSG000001	5	0.33796404	0.346207061
FOXL1	0.7404083	0	CLDN1,CSTA	ENSG000001	12	0.01028676	0.011676864
SP3	0.73631916	0	CCND1,CD9	ENSG000001	341	2.68E-23	1.87E-22
MAZ	0.73630729	0	CCND1,CD9	ENSG000001	154	1.10E-16	4.61E-16
ZFX	0.73398915	0	CCND1,CD9	ENSG000001	298	6.40E-24	8.96E-23
KLF3	0.73038837	0	CD9,CLDN1,	ENSG00000C	61	6.87E-10	1.70E-09
PATZ1	0.71325537	0	CCND1,CD9	ENSG000001	327	9.44E-24	9.91E-23
CPEB1	0.71276509	0	ABCC5,ALDH	ENSG000001	171	4.87E-20	2.56E-19
KLF12	0.70855985	0	CD9,KRT19,F	ENSG00000C	41	1.72E-06	2.92E-06
WT1	0.70841234	0	CD9,CLDN1,	ENSG00000C	172	3.70E-15	1.41E-14
AP2B	0.69876721	0	CD9,PERP,YE	ENSG00000C	47	5.04E-09	1.12E-08
PITX2	0.69671076	0	ABCC5,CD9,	ENSG000001	165	1.29E-19	6.00E-19
AP2D	0.69525839	0	PERP,ANXA2,	ENSG000001	39	4.74E-07	8.66E-07
ZN770	0.69448425	0	ABCC5,CCN	ENSG000001	342	1.02E-27	4.28E-26
SP2	0.69280813	0	CD9,CLDN1,	ENSG00000C	208	1.37E-23	1.15E-22
NR1I3	0.68838908	0	CD9,KRT19,F	ENSG00000C	12	0.00186911	0.002453209

ETV2	0.68817058	0	CD9,YBX3,C	ENSG00000(	6	0.00353352	0.004122438
BC11A	0.6865101	0	ANP32A,ANX	ENSG000001	49	3.85E-09	8.97E-09
ZN467	0.68550693	0	CCND1,CD9	ENSG000001	118	9.45E-12	2.83E-11
IRF3	0.67518949	0	ANXA2,AP2S1	ENSG000001	38	2.35E-07	4.49E-07
KLF6	0.67437735	0	DSP,ANXA2,A	ENSG00000(	18	0.01326835	0.014665017
KLF16	0.66937902	0	PERP,ANP32A	ENSG000001	60	8.50E-09	1.78E-08
EGR1	0.66603556	0	C1QBP,CCT6	ENSG000001	12	2.18E-05	3.39E-05
CTCFL	0.66500951	0	C1QBP,DSTN	ENSG000001	12	0.04208395	0.044188152
HXC10	0.66021501	0	CCT6A,CLNS	ENSG000001	11	7.75E-05	0.000112291
SALL4	0.65342477	0.0044	C1QBP,CCT6	ENSG000001	8	0.00308652	0.003703827
THA	0.65096712	0.0044	AURKAIP1,BC	ENSG000001	20	1.74E-06	2.92E-06
FOXJ3	0.64914222	0.0044	CLNS1A,DGL	ENSG00000(	9	6.85E-05	0.000102697
FLI1	0.64066426	0.0044	BCL3,C1QBP	ENSG00000(	16	1.87E-06	3.03E-06
ZSC22	0.63036273	0.0044	AP2S1,EIF1AX	ENSG00000(	9	0.00092616	0.001254804
PURA	0.7934459	0	AHCY,CLDN4	ENSG000001	9	0.03888145	0.043325044
ZN331	0.78974149	0	CLDN1,CLDN	ENSG000001	14	0.00714307	0.008705613
EGR2	0.78771082	0	AHCY,CLDN7	ENSG000001	17	0.00194989	0.002622265
HXC6	0.78192282	0	IGFBP2,KRT1	ENSG000001	8	0.28725806	0.287258056
NFAC1	0.77751381	0	IGFBP2,KRT1	ENSG000001	7	0.21534011	0.221006951
ZN320	0.76745364	0	IGFBP2,KRT1	ENSG000001	5	0.08941345	0.09686457
ZN148	0.76300208	0	AHCY,CLDN4	ENSG000001	20	0.00913461	0.010795449
ZN274	0.74687643	0	AHCY,CLDN7	ENSG000001	7	0.21534011	0.221006951
RARB	0.74347378	0	AHCY,CD9,C	ENSG000001	22	7.32E-05	0.000118944
XBP1	0.73479736	0	AHCY,MDK,P	ENSG000001	9	0.00092616	0.001290015
ANDR	0.7203007	0	CSTA,MDK,SI	ENSG000001	6	0.00353352	0.004445394
NFKB2	0.70357774	0	CSTA,MDK,IF	ENSG000001	5	0.01259944	0.014452295
FOXJ3	0.69490963	0	AHCY,CLDN7	ENSG000001	39	4.74E-07	8.41E-07
ZN257	0.69409863	0	AHCY,PERP,A	ENSG000001	22	1.16E-05	1.98E-05
TEAD1	0.67168615	0	AHCY,SPINT2	ENSG000001	5	0.00073306	0.001058861
KLF6	0.6557756	0	CD9,ACP1,AI	ENSG00000(	23	4.86E-08	9.02E-08
PRDM6	0.64960018	0	AHCY,CLDN7	ENSG000001	114	6.68E-11	1.63E-10
PAX5	0.64945564	0	MDK,SPINT2,	ENSG000001	53	1.36E-12	3.78E-12
SP2	0.64737238	0	AHCY,ATL2,C	ENSG000001	269	5.46E-21	2.13E-20
ETS2	0.6449121	0	AHCY,PERP,A	ENSG000001	146	6.23E-15	1.87E-14
SP4	0.63986265	0	AHCY,ARL5A,	ENSG000001	42	5.60E-10	1.29E-09
SP1	0.63962037	0	AHCY,ATL2,C	ENSG000001	315	1.30E-27	1.01E-26
TBX15	0.6377525	0	AHCY,CD9,C	ENSG000001	280	1.38E-22	6.72E-22
RXRA	0.63466274	0	AHCY,ATL2,P	ENSG000001	360	1.35E-29	1.32E-28
SP3	0.63419229	0	AHCY,PERP,F	ENSG000001	343	1.77E-22	7.69E-22
WT1	0.63191158	0	AHCY,AAMP,A	ENSG000001	181	5.06E-15	1.64E-14
THAP1	0.625813	0	AHCY,ACAP2	ENSG000001	88	1.92E-08	3.74E-08
MAZ	0.62573455	0	AHCY,RCN1,	ENSG000001	171	1.82E-16	6.46E-16
KLF1	0.62294002	0	ACP1,ARL5A,	ENSG000001	44	1.81E-08	3.72E-08
PATZ1	0.61973166	0	AHCY,C19or	ENSG000001	304	6.24E-30	8.12E-29
NRF1	0.61565928	0.0058	RCN1,ACAP2	ENSG00000(	103	1.58E-11	4.10E-11

VEZF1	0.61489233	0.0116	AHCY,APP,CI	ENSG000001	338	2.30E-26	1.49E-25
SALL4	0.61392539	0.0116	AHCY,PERP,A	ENSG000001	22	0.00038357	0.00057536
SRY	0.61238132	0.0174	CLNS1A,COF	ENSG00000(	24	0.000275	0.000428995
ZFX	0.60554469	0.029	AHCY,PERP,F	ENSG000001	382	7.16E-33	1.40E-31
ZSC22	0.60438862	0.029	COPS6,GTF2	ENSG000001	10	0.00245536	0.003191968
CPEB1	0.60088247	0.029	AHCY,CD9,C	ENSG000001	285	2.70E-24	1.50E-23
ZN770	0.6000474	0.029	AHCY,C19or	ENSG000001	651	1.34E-45	5.22E-44
KLF3	0.59598803	0.029	PERP,ACP1,A	ENSG000001	45	1.06E-09	2.30E-09
ZN768	0.82599808	0	AHNAK2,ATP	ENSG000001	47	0.43344311	0.688409653
E2F7	0.82365863	0	AHNAK2,CLC	ENSG000001	27	0.99353745	0.993537452
HXC12	0.81916198	0	CLCA2,COL1	ENSG000001	10	0.43245639	0.688409653
E2F1	0.81324753	0	CLCA2,DSC3	ENSG000001	16	0.98658925	0.993537452
HMX1	0.81310803	0	ATP1A1,CLCA	ENSG000001	17	0.19381561	0.523302159
SP4	0.81161075	0	ATP1A1,CLCA	ENSG000001	30	0.14943412	0.489057106
NFIC	0.80913021	0	ATP1A1,CLCA	ENSG000001	18	0.42586632	0.688409653
FLI1	0.80906707	0	AHNAK2,ATP	ENSG000001	45	0.64371122	0.78944487
E2F3	0.80886769	0	ATP1A1,CLCA	ENSG000001	22	0.62063893	0.783738096
ETV5	0.80731705	0	ATP1A1,CLCA	ENSG000001	14	0.42947929	0.688409653
HAND1	0.80667774	0	CLCA2,CXCL	ENSG000001	18	0.83403738	0.891841951
ZN148	0.80642227	0	AHNAK2,CLC	ENSG000001	23	0.93428094	0.960974681
STAT1	0.80597883	0	ATP1A1,COL1	ENSG000001	13	0.62408774	0.783738096
COT1	0.80567601	0	AHNAK2,ATP	ENSG000001	57	0.17030554	0.514842441
PRDM4	0.80522296	0	AHNAK2,ATP	ENSG000001	16	0.54382097	0.762761875
EGR2	0.80468881	0	ATP1A1,CXCI	ENSG000001	29	0.71307458	0.82808661
BC11A	0.80463555	0	ATP1A1,COL1	ENSG000001	17	0.59632898	0.777438619
ZN436	0.8034954	0	ATP1A1,CLCA	ENSG000001	21	0.20913835	0.537332855
RARA	0.80319163	0	ATP1A1,CLCA	ENSG000001	19	0.68967532	0.809618849
ZIC2	0.80314149	0	ATP1A1,CLCA	ENSG000001	23	0.66276322	0.78944487
ZN740	0.80263045	0	ATP1A1,CLCA	ENSG000001	24	0.51475237	0.758804345
RXRA	0.80258424	0	ATP1A1,CLCA	ENSG000001	30	0.14943412	0.489057106
NFAC1	0.80222952	0	AHNAK2,ATP	ENSG000001	16	0.76614701	0.880254007
TBX21	0.80177754	0	AHNAK2,CLC	ENSG000001	18	0.83403738	0.891841951
ONEC2	0.80151134	0	COL17A1,DS	ENSG00000(	8	0.88413909	0.918144437
KLF9	0.80100308	0	AHNAK2,ATP	ENSG000001	42	0.40438072	0.688409653
ZIC3	0.80069309	0	CLCA2,CXCL	ENSG000001	20	0.52770114	0.759889637
ZN563	0.80011383	0	CLCA2,COL1	ENSG000001	23	0.28927631	0.650871693
PO3F4	0.79977223	0	CLCA2,COL1	ENSG000001	9	0.6651804	0.78944487
VEZF1	0.79744969	0	ATP1A1,CLCA	ENSG000001	49	0.09578897	0.344840277
SUH	0.79684056	0	CXCL14,DAA	ENSG000001	11	0.50115515	0.758804345
ZN219	0.79490104	0	ATP1A1,COL1	ENSG000001	24	0.18622594	0.523302159
OLIG2	0.79201874	0	ATP1A1,CLCA	ENSG000001	15	0.26862876	0.617274595
TBX20	0.79176602	0	CLCA2,COL1	ENSG000001	17	0.59632898	0.777438619
LMX1A	0.78989059	0	CLCA2,CSTA	ENSG000001	11	0.50115515	0.758804345
MAZ	0.7895959	0	AHNAK2,ATP	ENSG000001	81	0.01679899	0.082467768
ETV2	0.78747837	0	ATP1A1,CLCA	ENSG000001	14	0.87740741	0.918144437

PURA	0.78696902	0	CLCA2,CXCL	ENSG000001	18	0.83403738	0.891841951
IRF3	0.78652464	0	CLCA2,CXCL	ENSG000001	10	0.43245639	0.688409653
ZN331	0.78635444	0	CLCA2,DSP,I	ENSG000001	15	0.98243951	0.993537452
PPARA	0.78551371	0	ATP1A1,CLC/	ENSG000001	20	0.1725963	0.514842441
NFIB	0.78432629	0	ATP1A1,CLC/	ENSG000001	12	0.56529463	0.772807853
TAL1	0.78373861	0	AHNAK2,DAA	ENSG000001	13	0.84880103	0.898730503
TEAD4	0.78360217	0	CLCA2,CXCL	ENSG000001	13	0.3693176	0.688409653
KLF15	0.78243609	0	AHNAK2,ATP	ENSG000001	71	0.00458524	0.03095036
Z324A	0.7816658	0	ATP1A1,CLC/	ENSG000001	13	0.17242972	0.514842441
ZN554	0.77954673	0	CXCL14,DAA	ENSG000001	13	0.06290705	0.242641471
ZN586	0.77950574	0	AHNAK2,COI	ENSG000001	21	0.20913835	0.537332855
THB	0.77901838	0	COL17A1,CX	ENSG000000	16	0.54382097	0.762761875
AP2C	0.77802788	0	CKAP4,COL1	ENSG000001	73	0.00156446	0.012997044
ZN263	0.77731947	0	ATP1A1,CLC/	ENSG000001	38	0.82705887	0.891841951
TBX15	0.77643158	0	AHNAK2,ATP	ENSG000001	120	0.0165132	0.082467768
ETS2	0.77415435	0	AHNAK2,ATP	ENSG000001	97	0.03756267	0.162270744
GATA3	0.77394554	0	ATP1A1,CLC/	ENSG000001	10	0.19263674	0.523302159
HEN1	0.77184935	0	CXCL14,DAA	ENSG000001	9	0.36051049	0.688409653
ARNT2	0.77096996	0	CXCL14,DSC	ENSG000001	13	0.62408774	0.783738096
ZN121	0.77072711	0	ATP1A1,CLC/	ENSG000001	14	0.21891339	0.537332855
TFDP1	0.77052457	0	CLCA2,DAAM	ENSG000001	8	0.59747598	0.777438619
ZSC31	0.77026317	0	CLCA2,COL1	ENSG000001	6	0.8013941	0.891841951
PRDM6	0.76848668	0	AHNAK2,ATP	ENSG000001	100	0.00661307	0.039678401
ZN281	0.76781096	0	ATP1A1,CLC/	ENSG000001	11	0.50115515	0.758804345
GLIS3	0.76714426	0	CXCL14,FSC	ENSG000001	10	0.43245639	0.688409653
ZSC22	0.76696225	0	CLCA2,COL1	ENSG000001	12	0.04208395	0.17481027
PAX5	0.76645503	0	ATP1A1,CLC/	ENSG000001	59	0.30800133	0.678860075
RARG	0.76609596	0	DAAM1,FSCN	ENSG000001	12	0.56529463	0.772807853
KLF12	0.76547991	0	ATP1A1,CLC/	ENSG000001	82	0.019897	0.093429376
ZF64A	0.76480509	0	ATP1A1,COL1	ENSG000001	11	0.24925968	0.585218381
PROX1	0.76397213	0	CXCL14,DSC	ENSG000001	9	0.6651804	0.78944487
ZBT17	0.76376392	0	ATP1A1,CLC/	ENSG000001	75	0.03572973	0.160783804
ZN467	0.763523	0	AHNAK2,ATP	ENSG000001	80	0.00080124	0.008653364
WT1	0.76341802	0	AHNAK2,ATP	ENSG000001	149	9.64E-06	0.000173442
MYNN	0.76304396	0	ATP1A1,CLC/	ENSG000001	31	0.17638121	0.514842441
FOXG1	0.7625451	0	CLCA2,DSG3	ENSG000001	9	0.6651804	0.78944487
EGR4	0.76218436	0	DAAM1,DSC3	ENSG000001	12	0.81422976	0.891841951
TBX1	0.7621267	0	AHNAK2,ATP	ENSG000001	117	0.0061424	0.039022335
ZN341	0.76143379	0	AHNAK2,ATP	ENSG000001	92	0.00135622	0.012205981
AP2D	0.76094644	0	ATP1A1,CLC/	ENSG000001	53	0.01487909	0.080347096
KLF5	0.76015982	0	CXCL14,DSC	ENSG000001	13	0.3693176	0.688409653
E2F4	0.75984618	0	ATP1A1,CLC/	ENSG000001	43	0.01450507	0.080347096
PBX1	0.75934114	0	CLCA2,CXCL	ENSG000001	7	0.5199215	0.758804345
HES1	0.75856708	0	ATP1A1,CXCI	ENSG000001	16	0.06080204	0.242641471
PATZ1	0.75598043	0	AHNAK2,ATP	ENSG000001	262	4.74E-06	0.000102301

KLF6	0.75433644	0	ATP1A1,CLC/	ENSG000001	34	0.41116353	0.688409653
GFI1	0.75199605	0	CXCL14,FSC	ENSG000001	6	0.43289824	0.688409653
AP2B	0.75125433	0	ATP1A1,C19c	ENSG000001	111	0.00400603	0.028843383
TFE2	0.74627936	0	CXCL14,FSC	ENSG000001	7	0.21534011	0.537332855
ZN335	0.74339952	0	DAAM1,FSCN	ENSG000001	9	0.36051049	0.688409653
TBX5	0.74224506	0	COL17A1,DS	ENSG00000(	6	0.8013941	0.891841951
SRBP2	0.74223216	0	DSG3,FSCN1	ENSG000001	9	0.36051049	0.688409653
FOXJ3	0.74111179	0	ATP1A1,COL1	ENSG000001	24	0.51475237	0.758804345
SP1	0.74066855	0	AHNAK2,ATP	ENSG000001	288	1.87E-08	5.05E-07
MECP2	0.74009359	0	ATP1A1,FSCN	ENSG000001	5	0.33796404	0.688409653
PRDM1	0.73960064	0	CXCL14,DSG	ENSG000001	8	0.09547686	0.344840277
KLF3	0.73620907	0	AHNAK2,ATP	ENSG000001	158	0.00288194	0.022232101
ZIC4	0.73390431	0	FSCN1,KRT1-	ENSG00000(	8	0.59747598	0.777438619
KLF16	0.73047746	0	CXCL14,DAA	ENSG000001	78	0.00108857	0.010687741
CPEB1	0.72999797	0	AHNAK2,ATP	ENSG000001	194	0.00036238	0.004348515
ZFX	0.72970245	0	ATP1A1,C19c	ENSG000001	148	7.22E-05	0.000975204
MXI1	0.72957963	0	CXCL14,FSC	ENSG000001	11	0.24925968	0.585218381
SP3	0.72835416	0	AHNAK2,ATP	ENSG000001	252	1.51E-12	1.63E-10
NR1H2	0.7272267	0	DAAM1,ITGA6	ENSG000001	6	0.43289824	0.688409653
ZN770	0.72284577	0	AHNAK2,ATP	ENSG000001	293	3.02E-10	1.09E-08
NR4A1	0.72270667	0	CXCL14,KRT	ENSG000001	5	0.33796404	0.688409653
ESR1	0.72222152	0	DAAM1,FSCN	ENSG000001	6	0.14809562	0.489057106
SP2	0.71847469	0	AHNAK2,ATP	ENSG000001	261	1.24E-10	6.70E-09
TAF1	0.71600439	0	AHNAK2,CKA	ENSG000001	98	1.96E-05	0.000302476
HXC10	0.67967451	0	AHNAK2,ATP	ENSG000001	38	0.40771867	0.688409653
KLF4	0.67099778	0	DAAM1,CAVI	ENSG000001	5	0.33796404	0.688409653
KLF1	0.74846449	0	ABCC5,ANAF	ENSG000001	105	1.49E-06	3.19E-06
ZN148	0.74479747	0	ABCC5,ANAF	ENSG000001	104	1.31E-07	3.28E-07
KLF3	0.74443956	0	ABCC5,ANAF	ENSG000001	70	0.00165428	0.002067847
E2F1	0.73399479	0	ABCC5,ANAF	ENSG000001	61	0.00078996	0.00103038
GATA3	0.72591576	0	ABCC5,ANAF	ENSG000001	59	0.00015448	0.000257473
RXRA	0.72326141	0	ABCC5,ANAF	ENSG000001	185	4.09E-10	1.12E-09
GABPA	0.72274617	0	ABCC5,COX5	ENSG000001	44	0.01854948	0.01987444
ZFX	0.7211015	0	ABCC5,ANAF	ENSG000001	141	4.70E-11	1.57E-10
MAZ	0.7209472	0	ABCC5,ANAF	ENSG000001	127	1.84E-06	3.46E-06
TBX15	0.712772	0	ABCC5,ANAF	ENSG000001	98	1.96E-05	3.46E-05
ZN263	0.71224119	0	ANAPC11,CC	ENSG000001	16	0.154691	0.154690999
ETS2	0.7103182	0	ABCC5,ANAF	ENSG000001	130	1.79E-06	3.46E-06
PATZ1	0.70738916	0	ABCC5,ANAF	ENSG000001	164	1.71E-12	6.42E-12
WT1	0.70656055	0	ABCC5,ANAF	ENSG000001	91	6.82E-07	1.57E-06
KLF15	0.70639861	0	ABCC5,DNAJ	ENSG000001	18	0.04184485	0.043287777
VEZF1	0.70489401	0	ABCC5,ANAF	ENSG000001	199	7.79E-14	3.34E-13
MBD2	0.70450651	0	ABCC5,ANAF	ENSG000001	66	0.00055316	0.000829745
SP1	0.70333641	0	ABCC5,ANAF	ENSG000001	198	1.55E-16	1.55E-15
KLF16	0.6997851	0	ABCC5,ANAF	ENSG000001	119	1.84E-10	5.51E-10

SP2	0.69871584	0	ABCC5,ANAF	ENSG000001	224	2.01E-15	1.21E-14
BC11A	0.69760201	0	COX5B,EMP2	ENSG000001	21	0.00020017	0.000316056
PRDM6	0.69737846	0	ABCC5,EIF2S	ENSG000001	36	0.0124081	0.013999375
FOXJ3	0.69686076	0	ABCC5,ANAF	ENSG000001	54	0.00060015	0.000857355
SP3	0.69510976	0	ABCC5,ANAF	ENSG000001	184	1.82E-14	9.08E-14
ZN121	0.6882075	0	EIF2S2,KRT1S	ENSG000001	5	0.01259944	0.013999375
ZN770	0.68474449	0	ABCC5,ANAF	ENSG000001	295	1.09E-26	3.26E-25
ELK1	0.65875178	0	COX5B,DNAJ	ENSG000001	26	0.00970507	0.011646079
CPEB1	0.65794375	0	ABCC5,ANAF	ENSG000001	144	5.72E-16	4.29E-15
PITX2	0.65322197	0	ABCC5,BEX3	ENSG000001	137	1.13E-17	1.70E-16
TEAD1	0.64672156	0	EIF2S2,PLD3	ENSG000001	23	0.00069194	0.000943553
ELK4	0.84287852	0	DSP,FXYD3,J	ENSG000000	14	0.67716278	0.804956527
KLF1	0.8424358	0	DSP,FXYD3,J	ENSG000000	19	0.13911423	0.403897159
ETV7	0.83982834	0	DSP,JUP,KRT	ENSG000000	11	0.09354659	0.300685465
ETV2	0.83770548	0	CDH1,DSP,F	ENSG000000	16	0.32041865	0.589627285
ZN467	0.83641804	0	DSP,FXYD3,J	ENSG000000	13	0.3693176	0.589627285
ZBT17	0.83622984	0	CDH1,DSG3	ENSG000000	20	0.52770114	0.730663113
KLF6	0.83554867	0	DSC3,DSP,F	ENSG000001	25	0.73741505	0.809357979
ZN148	0.83517988	0	DSP,F11R,FX	ENSG000000	19	0.68967532	0.804956527
RXRA	0.83471473	0	CDH1,DSC3	ENSG000000	28	0.19688425	0.478907645
MYOG	0.82928353	0	DSP,FXYD3,J	ENSG000000	8	0.59747598	0.74684497
NFAC1	0.82900831	0	CBR1,DSP,F)	ENSG000001	15	0.72446087	0.804956527
KLF15	0.82739724	0	CBR1,CDH3	ENSG000001	39	0.92540347	0.946423459
ZN740	0.82737871	0	DSP,JUP,KRT	ENSG000000	17	0.59632898	0.74684497
COT1	0.82690899	0	CBR1,CDH1	ENSG000001	47	0.81258964	0.842306644
TBX1	0.82612433	0	DSG3,DSP,F	ENSG000001	40	0.93590764	0.946423459
FLI1	0.82558502	0	CDH1,DSC3	ENSG000000	35	0.18448241	0.474383351
KLF16	0.82498151	0	CDH1,DSC3	ENSG000000	23	0.66276322	0.804956527
GATA2	0.82412542	0	CDH1,DSG3	ENSG000000	30	0.94698034	0.946980341
ZN350	0.82401873	0	CBR1,DSP,F	ENSG000001	17	0.80253658	0.842306644
TEAD1	0.82334553	0	DSP,FXYD3,J	ENSG000000	12	0.81422976	0.842306644
FUBP1	0.82293189	0	CDH1,DSP,F	ENSG000000	12	0.30873671	0.589627285
RREB1	0.82279608	0	DSP,FXYD3,J	ENSG000000	10	0.7233614	0.804956527
PAX5	0.82234827	0	DSP,FXYD3,J	ENSG000000	16	0.54382097	0.741574045
ANDR	0.82053409	0	CDH1,DSP,F	ENSG000000	17	0.59632898	0.74684497
ZNF76	0.82036753	0	DSP,JUP,KRT	ENSG000000	9	0.36051049	0.589627285
ZN331	0.8178975	0	DSP,JUP,KRT	ENSG000000	9	0.14075318	0.403897159
SRBP2	0.81764547	0	DSP,JUP,KRT	ENSG000000	12	0.56529463	0.74684497
MAZ	0.81689646	0	CDH1,DSC3	ENSG000000	31	0.62264218	0.767641045
ZSCA4	0.8164808	0	KRT17,MIR20	ENSG000001	5	0.33796404	0.589627285
SALL4	0.81242696	0	CBR1,DSP,F	ENSG000001	33	0.37343061	0.589627285
E2F6	0.8119281	0	CBR1,CDH1	ENSG000001	38	0.27249093	0.589627285
ELF5	0.81150981	0	JUP,KRT17,KF	ENSG000001	12	0.81422976	0.842306644
SP4	0.81134954	0	DSP,JUP,KRT	ENSG000000	20	0.07693324	0.276959654
ZN281	0.81006162	0	CBR1,DSP,F	ENSG000001	24	0.70171344	0.804956527

KLF12	0.80985377	0	CBR1,DSP,F)	ENSG000001	38	0.27249093	0.589627285
ZN586	0.80849739	0	DSP,JUP,KRT:	ENSG00000(	8	0.28725806	0.589627285
NFYB	0.80836772	0	CDH1,F11R,.	ENSG00000(	9	0.36051049	0.589627285
ZN121	0.80830539	0	JUP,KRT17,KI	ENSG000001	10	0.19263674	0.478907645
TBX15	0.80798689	0	CBR1,CDH1.	ENSG000001	67	0.09153379	0.300685465
KLF5	0.80777103	0	CBR1,DSP,JU	ENSG000001	13	0.3693176	0.589627285
KLF3	0.80690192	0	DSP,F11R,FX	ENSG00000(	28	0.33439824	0.589627285
PRDM6	0.80370044	0	CBR1,CDH1.	ENSG000001	58	0.07201581	0.270059289
FOXJ3	0.80250096	0	CBR1,CDH1.	ENSG000001	87	0.00017703	0.001333369
AP2B	0.79942768	0	DSP,FXYD3,K	ENSG00000(	10	0.7233614	0.804956527
HXC10	0.79877517	0	DSP,JUP,PER	ENSG00000(	8	0.28725806	0.589627285
PTF1A	0.79873235	0	KRT17,KRT5,I	ENSG000001	6	0.43289824	0.649347363
SMAD1	0.79769839	0	JUP,KRT17,PI	ENSG000001	9	0.03888145	0.18417529
ETS2	0.79742854	0	CDH1,DSP,F	ENSG00000(	133	0.00079203	0.005483282
MAFF	0.79501538	0	KRT17,KRT5,S	ENSG000001	6	0.14809562	0.403897159
WT1	0.79421634	0	CBR1,DSC3,	ENSG000001	213	1.27E-05	0.00011441
GATA3	0.79288187	0	KRT5,PERP,SI	ENSG000001	5	0.33796404	0.589627285
KLF4	0.79188145	0	DSP,JUP,KRT	ENSG00000(	17	0.37316991	0.589627285
PATZ1	0.79157901	0	C16orf74,CB	ENSG000001	235	0.00017778	0.001333369
TFE2	0.78961795	0	KRT17,KRT5,I	ENSG000001	6	0.43289824	0.649347363
ZN263	0.7880828	0	CLCA2,DHCI	ENSG000001	303	1.09E-14	1.40E-13
RARB	0.78731832	0	CBR1,KRT14.	ENSG000001	12	0.30873671	0.589627285
ZBTB4	0.78679769	0	DSP,FXYD3,J	ENSG00000(	11	0.77274057	0.83791146
ITF2	0.78664736	0	KRT17,KRT5,I	ENSG000001	7	0.5199215	0.730663113
PLAL1	0.78630051	0	DSP,JUP,KRT	ENSG00000(	7	0.5199215	0.730663113
VEZF1	0.7859592	0	CDH1,DSC3.	ENSG00000(	390	3.64E-09	3.64E-08
ZFX	0.78528909	0	C16orf74,CL	ENSG000001	539	3.48E-23	1.04E-21
SP2	0.78357816	0	CALML3,CBR	ENSG000001	601	1.76E-22	3.96E-21
ZN770	0.78194727	0	ALDH3A1,C1	ENSG000001	845	2.71E-30	2.44E-28
SRY	0.78055266	0	DSP,F11R,PT	ENSG00000(	9	0.36051049	0.589627285
SP3	0.7798116	0	CALML3,CBR	ENSG000001	655	5.55E-27	2.50E-25
PITX2	0.77946581	0	CBR1,CDH1.	ENSG000001	232	5.51E-10	6.19E-09
AP2D	0.77932572	0	CBR1,DSP,JU	ENSG000001	17	0.02914418	0.154292735
IRF3	0.77650523	0	DSG3,DSP,F	ENSG000001	23	0.46899148	0.691954649
AP2C	0.77636637	0	DSP,S100A1(	ENSG00000(	5	0.08941345	0.300685465
Z324A	0.77601127	0	JUP,KRT5,PEI	ENSG000001	5	0.33796404	0.589627285
SP1	0.77526657	0	CBR1,CDH1.	ENSG000001	450	3.03E-17	5.46E-16
CPEB1	0.7752047	0	CBR1,CDH1.	ENSG000001	391	6.23E-15	9.34E-14
ZN219	0.77204051	0	CDH1,KRT17	ENSG00000(	16	0.00496917	0.029815022
RUNX2	0.76968426	0	DSP,F11R,MI	ENSG00000(	7	0.05843632	0.239057658
ESR2	0.76870034	0	KRT5,PERP,SI	ENSG000001	6	0.14809562	0.403897159
MYF6	0.765671	0	FXYD3,KRT5,	ENSG00000(	7	0.05843632	0.239057658
ZN341	0.76488233	0	CDH1,DSP,F	ENSG00000(	43	0.03165321	0.158266036
EGR4	0.7635133	0	CBR1,NME1,	ENSG000001	13	0.17242972	0.456431608
STAT3	0.76202758	0	DSP,KRT5,S1	ENSG00000(	7	0.5199215	0.730663113

ETV6	0.76007715	0	JUP,KRT5,PEI	ENSG000001	6	0.43289824	0.649347363
VDR	0.7576645	0	CBR1,KRT14,	ENSG000001	8	0.59747598	0.74684497
ZN143	0.75486174	0	DSP,F11R,KR	ENSG00000(	13	0.06290705	0.246158014
PO4F1	0.74716233	0	PERP,SLC2A1	ENSG000001	5	0.33796404	0.589627285
THA11	0.74512781	0	PERP,SDC1,S	ENSG000001	7	0.05843632	0.239057658
P63	0.74489923	0	CBR1,S100A	ENSG000001	5	0.01259944	0.070871833
ZN768	0.73441591	0	KRT5,NME1,S	ENSG000001	8	0.59747598	0.74684497
PURA	0.73259489	0	JUP,PERP,S1(	ENSG000001	7	0.21534011	0.510016041
TAF1	0.73238578	0	JUP,PERP,S1(	ENSG000001	17	0.00194989	0.012535001
FOXC2	0.73093627	0	NME1,SLC2A	ENSG000002	6	0.14809562	0.403897159
ZF64A	0.72961689	0	KRT14,NME1	ENSG000001	10	0.7233614	0.804956527

_Q_FDR_value

Table S2

88TFs identified from HNSCC patient scRNA-seq datasets

PATZ1
SP1
SP2
SP3
ZFX
ZN770
VEZF1
WT1
CPEB1
MAZ
ETS2
TBX15
RXRA
SP4
PITX2
FOXJ3
KLF16
KLF3
PRDM6
ZN467
AP2B
KLF12
KLF6
RARB
SALL4
TAF1
TBX1
TEAD1
ZN341
AP2D
FLI1
KLF15
THA
ZN148
ZSC22
ANDR
BC11A
E2F7
GATA3
HXC10
IRF3
KLF1
KLF5

NR1I3
NRF1
PAX5
THAP1
ZN219
ZN263
ZN281
AP2C
ASCL1
CTCFL
E2F1
E2F6
EGR1
GATA2
EGR2
EGR4
ELK1
ESR2
ETV2
ETV5
FOXL1
FUBP1
GABPA
GATA4
HXD13
ITF2
MAFA
MBD2
MEF2B
NFAC1
NFKB2
PURA
RARA
RFX1
RXRB
SRY
TBX5
VDR
XBP1
ZBT17
ZN121
ZN257
ZN331
ZN586
ZN740

Table S3

regulated_genes	TF
CBR1	PRDM6
CDH1	PRDM6
DSC3	PRDM6
DSG3	PRDM6
DSP	PRDM6
F11R	PRDM6
FXYD3	PRDM6
JUP	PRDM6
KRT17	PRDM6
KRT5	PRDM6
KRT6A	PRDM6
LAMC2	PRDM6
MIR205HG	PRDM6
NME1	PRDM6
PERP	PRDM6
PKP1	PRDM6
PTPRF	PRDM6
RBP1	PRDM6
S100A16	PRDM6
SDC1	PRDM6
SFN	PRDM6
SLC2A1	PRDM6
SPINT2	PRDM6
TACSTD2	PRDM6
TP63	PRDM6
ACAP2	PRDM6
AP1G1	PRDM6
AP2S1	PRDM6
ARPC1A	PRDM6
ATG12	PRDM6
BAG1	PRDM6
BCL6	PRDM6
CCT8	PRDM6
EIF4EBP1	PRDM6
EML4	PRDM6
FSCN1	PRDM6
GTF3A	PRDM6
HILPDA	PRDM6
LRRC59	PRDM6
MAP1B	PRDM6
MYO6	PRDM6
NANS	PRDM6
NOTCH3	PRDM6

PLS3	PRDM6
PTK2	PRDM6
SCPEP1	PRDM6
SDHC	PRDM6
SH3BGRL	PRDM6
SNAP23	PRDM6
SNRPC	PRDM6
SNRPE	PRDM6
TAF1D	PRDM6
TMTC3	PRDM6
TTC17	PRDM6
USP11	PRDM6
VAMP8	PRDM6
ZFC3H1	PRDM6
ZFP64	PRDM6
ABCC5	PRDM6
EIF2S2	PRDM6
EMP2	PRDM6
KRT19	PRDM6
MLF2	PRDM6
PLD3	PRDM6
SEM1	PRDM6
TM4SF1	PRDM6
BANF1	PRDM6
BST2	PRDM6
CAPN1	PRDM6
CAPNS1	PRDM6
CNBP	PRDM6
COX7B	PRDM6
CPNE1	PRDM6
GLUL	PRDM6
OTUB1	PRDM6
PDIA3	PRDM6
PGAM1	PRDM6
PSMB1	PRDM6
PSMB4	PRDM6
RAC1	PRDM6
RACK1	PRDM6
RPL15	PRDM6
RPL41	PRDM6
RPL6	PRDM6
SEC62	PRDM6
SSR2	PRDM6
SYNGR2	PRDM6
TMA7	PRDM6

TMEM258	PRDM6
TNFSF10	PRDM6
TUBA1C	PRDM6
UBL5	PRDM6
AHNAK2	PRDM6
ATP1A1	PRDM6
CLCA2	PRDM6
COL17A1	PRDM6
CXCL14	PRDM6
DAAM1	PRDM6
DST	PRDM6
FGFBP1	PRDM6
GJB2	PRDM6
ITGA6	PRDM6
KRT14	PRDM6
KRT6B	PRDM6
MAPK6	PRDM6
PRRG4	PRDM6
PTPRZ1	PRDM6
S100A14	PRDM6
S100A2	PRDM6
AHNAK	PRDM6
AIMP1	PRDM6
ASCC3	PRDM6
ASPM	PRDM6
ATOX1	PRDM6
ATP1B3	PRDM6
BSG	PRDM6
C1orf21	PRDM6
CAV1	PRDM6
CAVIN1	PRDM6
CCT3	PRDM6
CENPE	PRDM6
CENPF	PRDM6
CKAP2	PRDM6
CLTB	PRDM6
CSTB	PRDM6
DDX60	PRDM6
DLGAP5	PRDM6
DYNC1H1	PRDM6
EIF1AY	PRDM6
EIF2AK2	PRDM6
EIF4A3	PRDM6
FUS	PRDM6
GNL3	PRDM6

HES1	PRDM6
HSBP1	PRDM6
IFI35	PRDM6
KIF20B	PRDM6
KPNA2	PRDM6
KRT6C	PRDM6
MAF	PRDM6
MAP4	PRDM6
MAPKAP1	PRDM6
MARCKS	PRDM6
MKI67	PRDM6
MRPL51	PRDM6
MRPL52	PRDM6
MZT2A	PRDM6
NHP2	PRDM6
NMI	PRDM6
NUSAP1	PRDM6
PHF14	PRDM6
PLP2	PRDM6
PRR11	PRDM6
PSMA3	PRDM6
PSMB7	PRDM6
PSMC6	PRDM6
PYCARD	PRDM6
RAB10	PRDM6
ROCK2	PRDM6
RPS4Y1	PRDM6
SAMD9	PRDM6
SBDS	PRDM6
SIGMAR1	PRDM6
SNRPB	PRDM6
TARS	PRDM6
TCEAL4	PRDM6
TCEAL9	PRDM6
TOP2A	PRDM6
TPX2	PRDM6
TRIP11	PRDM6
TTC3	PRDM6
UBE2K	PRDM6
UQCRC1	PRDM6
VRK2	PRDM6
WDR43	PRDM6
YBX3	PRDM6
YLPM1	PRDM6
ZNF326	PRDM6

AHCY	PRDM6
CLDN1	PRDM6
CSTA	PRDM6
IGFBP2	PRDM6
KRT8	PRDM6
MDK	PRDM6
PDLIM1	PRDM6
RCN1	PRDM6
AKAP9	PRDM6
ARF1	PRDM6
ARL5A	PRDM6
ATIC	PRDM6
BPTF	PRDM6
C9orf78	PRDM6
CAMTA1	PRDM6
CD59	PRDM6
CDC123	PRDM6
CDK4	PRDM6
CLNS1A	PRDM6
COA4	PRDM6
COPS6	PRDM6
COPZ1	PRDM6
CYCS	PRDM6
DARS	PRDM6
DCAF7	PRDM6
DDX18	PRDM6
DDX46	PRDM6
DSTN	PRDM6
DYNLT1	PRDM6
EIF1AX	PRDM6
EIF4A2	PRDM6
EIF4E	PRDM6
EIF5B	PRDM6
ELAVL1	PRDM6
EMC4	PRDM6
ETFA	PRDM6
G3BP1	PRDM6
GLTP	PRDM6
GRSF1	PRDM6
GTF2I	PRDM6
HACD3	PRDM6
HDLBP	PRDM6
HM13	PRDM6
HNRNPA0	PRDM6
HNRNPD	PRDM6

HNRNPH3	PRDM6
HSPA9	PRDM6
IDH1	PRDM6
ILF2	PRDM6
ITGB1	PRDM6
LRPPRC	PRDM6
LSM4	PRDM6
LSM6	PRDM6
LYPLA1	PRDM6
MEAF6	PRDM6
METTL5	PRDM6
MIEN1	PRDM6
MMADHC	PRDM6
MPHOSPH8	PRDM6
MRFAP1	PRDM6
MRPL4	PRDM6
MRPS34	PRDM6
NDUFA10	PRDM6
NDUFA5	PRDM6
NDUFA8	PRDM6
NDUFB4	PRDM6
NDUFS3	PRDM6
NDUFS5	PRDM6
NDUFV1	PRDM6
NFE2L2	PRDM6
NT5C	PRDM6
NUDC	PRDM6
PDAP1	PRDM6
PFDN2	PRDM6
PGLS	PRDM6
PHB	PRDM6
POLR2G	PRDM6
PRDX3	PRDM6
PRELID1	PRDM6
PRMT1	PRDM6
PSMA4	PRDM6
PSMC2	PRDM6
PSMD11	PRDM6
PSMD4	PRDM6
RBM4	PRDM6
RCN2	PRDM6
RPN2	PRDM6
RSBN1L	PRDM6
SNU13	PRDM6
SRSF1	PRDM6

SRSF9	PRDM6
SSB	PRDM6
TFG	PRDM6
THOC3	PRDM6
TIMM13	PRDM6
TMBIM4	PRDM6
TMEM230	PRDM6
TMEM30A	PRDM6
TXNDC12	PRDM6
UBA2	PRDM6
VDAC3	PRDM6
XRN2	PRDM6
ZCRB1	PRDM6
PGRMC1	PRDM6
SOX4	PRDM6
ANXA2	PRDM6
ATRX	PRDM6
C1QBP	PRDM6
CCT2	PRDM6
CLTA	PRDM6
ERGIC3	PRDM6
GSTP1	PRDM6
NDUFAB1	PRDM6
NUCKS1	PRDM6
PPA1	PRDM6
PRDX2	PRDM6
SNRPF	PRDM6
SUPT4H1	PRDM6
UGDH	PRDM6
KRT18	PRDM6
NUPR1	PRDM6
SGK1	PRDM6
ADH5	PRDM6
AKR1A1	PRDM6
ANAPC5	PRDM6
BNIP3L	PRDM6
BUB3	PRDM6
CAPRIN1	PRDM6
COA3	PRDM6
CST3	PRDM6
DCTN2	PRDM6
DUT	PRDM6
FAM162A	PRDM6
H2AFY	PRDM6
HDAC2	PRDM6

IER3IP1	PRDM6
IVNS1ABP	PRDM6
MED10	PRDM6
NBEAL1	PRDM6
NR4A1	PRDM6
OLA1	PRDM6
PGD	PRDM6
PSMG1	PRDM6
RABGGTB	PRDM6
RBBP4	PRDM6
RBCK1	PRDM6
RTN4	PRDM6
STMN1	PRDM6
TMSB4X	PRDM6
TPGS2	PRDM6
TXN2	PRDM6
BCL7A	PRDM6
C6orf141	PRDM6
CALD1	PRDM6
CLDN7	PRDM6
CNN3	PRDM6
COL4A2	PRDM6
EDARADD	PRDM6
ELF3	PRDM6
EPCAM	PRDM6
FABP6	PRDM6
FERMT1	PRDM6
HOOK2	PRDM6
IRF6	PRDM6
JMJD4	PRDM6
KCNK1	PRDM6
KRTCAP3	PRDM6
MAL2	PRDM6
NPPC	PRDM6
PAWR	PRDM6
PRRX1	PRDM6
RAB25	PRDM6
RAI14	PRDM6
SOX2	PRDM6
ACBD3	PRDM6
ACBD6	PRDM6
AFG3L2	PRDM6
AHCTF1	PRDM6
ANKRD39	PRDM6
APP	PRDM6

ARPC1B	PRDM6
ATL2	PRDM6
BCAT2	PRDM6
BCL2	PRDM6
BMS1	PRDM6
BOD1	PRDM6
BPHL	PRDM6
C12orf73	PRDM6
C1orf105	PRDM6
CCDC25	PRDM6
CENPH	PRDM6
CERS4	PRDM6
COLGALT1	PRDM6
COTL1	PRDM6
CRB3	PRDM6
CROT	PRDM6
CTNND1	PRDM6
DCAF6	PRDM6
DDX56	PRDM6
DERA	PRDM6
DNAJC10	PRDM6
DNM1L	PRDM6
EBPL	PRDM6
ECE2	PRDM6
EIF2AK4	PRDM6
EIF2B5	PRDM6
ERI3	PRDM6
EXOSC5	PRDM6
FAM210B	PRDM6
FAM71D	PRDM6
FBLN1	PRDM6
FUNDC1	PRDM6
GAMT	PRDM6
GCDH	PRDM6
GDE1	PRDM6
GPATCH4	PRDM6
HBS1L	PRDM6
HEATR1	PRDM6
HLA-DQA1	PRDM6
HMGB3	PRDM6
HOMER3	PRDM6
HSPG2	PRDM6
IARS	PRDM6
IARS2	PRDM6
LAD1	PRDM6

LCMT1	PRDM6
LPGAT1	PRDM6
LSR	PRDM6
MAGED1	PRDM6
MAGEF1	PRDM6
MID1IP1	PRDM6
MLST8	PRDM6
MPZL1	PRDM6
NET1	PRDM6
NFIC	PRDM6
NIPSNAP1	PRDM6
NMD3	PRDM6
NR2C2AP	PRDM6
OGFRL1	PRDM6
OSBPL1A	PRDM6
PDHX	PRDM6
PKN2	PRDM6
PLTP	PRDM6
PON2	PRDM6
PPP1R35	PRDM6
PRR14L	PRDM6
PYCR1	PRDM6
QTRT1	PRDM6
RAMP1	PRDM6
RFC2	PRDM6
RNASEH1	PRDM6
S100A4	PRDM6
SEH1L	PRDM6
SENP2	PRDM6
SENP5	PRDM6
SLC5A6	PRDM6
SMARCD2	PRDM6
SORD	PRDM6
STAR	PRDM6
STARD10	PRDM6
TARBP1	PRDM6
TCTEX1D2	PRDM6
TGIF2	PRDM6
THUMPD1	PRDM6
TMEM167B	PRDM6
TMEM41A	PRDM6
TP53TG1	PRDM6
TPD52	PRDM6
TPRA1	PRDM6
TRIP6	PRDM6

UCHL5	PRDM6
VCAM1	PRDM6
VIM	PRDM6
YDJC	PRDM6
ZFPL1	PRDM6
ZNF581	PRDM6
ZNF90	PRDM6
CALML3	PRDM6
EGFR	PRDM6
GPX2	PRDM6
ITGA2	PRDM6
NFIA	PRDM6
NRXN1	PRDM6
PCDH7	PRDM6
RND3	PRDM6
SMAD1	PRDM6
AACS	PRDM6
ANKRD17	PRDM6
ANKRD65	PRDM6
ATXN7L3B	PRDM6
BCL11A	PRDM6
BRD3	PRDM6
CHCHD6	PRDM6
COA1	PRDM6
DDX27	PRDM6
DHX29	PRDM6
FBXO25	PRDM6
FOXA1	PRDM6
GALNT11	PRDM6
GLRX5	PRDM6
GNG12	PRDM6
GOT2	PRDM6
GPATCH2	PRDM6
HSPA4L	PRDM6
IGSF9	PRDM6
KHSRP	PRDM6
KIAA1522	PRDM6
KXD1	PRDM6
LAPTM4B	PRDM6
LRRC58	PRDM6
LUZP1	PRDM6
MECOM	PRDM6
MKKS	PRDM6
MMP14	PRDM6
MPST	PRDM6

MTR	PRDM6
MTUS1	PRDM6
NF1	PRDM6
POGZ	PRDM6
POLR2C	PRDM6
PPP4R2	PRDM6
RBBP8	PRDM6
RNF126	PRDM6
RPAP2	PRDM6
SIX1	PRDM6
SLC25A4	PRDM6
SMARCD1	PRDM6
SSBP3	PRDM6
TFF3	PRDM6
TPM1	PRDM6
TRAF4	PRDM6
TRIM29	PRDM6
ZBTB18	PRDM6
ZNF131	PRDM6
ABCA13	PRDM6
FZD6	PRDM6
KIAA1217	PRDM6
PTGES	PRDM6
ABHD17C	PRDM6
ACKR3	PRDM6
ARFGEF1	PRDM6
ARHGAP29	PRDM6
ARL4A	PRDM6
ATF5	PRDM6
C1orf122	PRDM6
CDC42EP3	PRDM6
CISD1	PRDM6
CMAS	PRDM6
COPS5	PRDM6
DAZAP1	PRDM6
ECE1	PRDM6
EPAS1	PRDM6
EXOC7	PRDM6
FADD	PRDM6
FAF1	PRDM6
FIP1L1	PRDM6
FRMD4A	PRDM6
FZD3	PRDM6
GABARAPL1	PRDM6
GADD45A	PRDM6

GOLPH3	PRDM6
GOSR1	PRDM6
GSTA4	PRDM6
IRF2BP2	PRDM6
ITGB6	PRDM6
ITPRIPL2	PRDM6
LAMB3	PRDM6
LGALS8	PRDM6
NUB1	PRDM6
NUFIP2	PRDM6
PHACTR4	PRDM6
PITHD1	PRDM6
PLEKHA5	PRDM6
PPFIA1	PRDM6
RBMS1	PRDM6
REPIN1	PRDM6
RERE	PRDM6
ROBO1	PRDM6
SEMA4B	PRDM6
SH2D4A	PRDM6
SMARCA4	PRDM6
SMC5	PRDM6
SRCAP	PRDM6
SRD5A3	PRDM6
STRBP	PRDM6
TMEM150C	PRDM6
TMEM159	PRDM6
TMEM87A	PRDM6
TRIO	PRDM6
UBR5	PRDM6
UBXN6	PRDM6
VGLL4	PRDM6
YBEY	PRDM6

Table S4

For RT-qPCR

GAPDH-F	GCCTCTTGTCTCTTAGATTTGGTC
GAPDH-R	TAGCACTCACCATGTAGTTGAGGT
PRDM6-F-1	GCCACCACTGCACTTAGAA
PRDM6-R_1	CCATCAACCTCTGTGGGAATAA
PRDM6_F_2	CTCCTGGTCATGAAAGTAGTAAGG
PRDM6_R_2	CACTTAGGGCAGGGAATTGT
IFITM1-F	TCTCACTGAGCACCGTCCCAGCATCCGGACA
IFITM1-R	TTCCTCCTTGTGCATCTTCTGGCTTTGGGGAAGGAAGTGTTGAG
ISG15-F	CTCTGAGCATCCTGGTGAGGAA
ISG15-R	AAGGTCAGCCAGAACAGGTCGT
E6-F	CTGCAATGTTTCAGGACCCA
E6-R	TCATGTATAGTTGTTTGCAGCTCTGT
E7-F	AAGTGTGACTCTACGCTTCGGTT
E7-R	GCCCATTAACAGGTCTTCCAAA